

University of Louisville

ThinkIR: The University of Louisville's Institutional Repository

Electronic Theses and Dissertations

12-2005

Optimization of process parameters for direct metal deposition of nickel.

Steven James Gravatte
University of Louisville

Follow this and additional works at: <https://ir.library.louisville.edu/etd>

Recommended Citation

Gravatte, Steven James, "Optimization of process parameters for direct metal deposition of nickel." (2005). *Electronic Theses and Dissertations*. Paper 525.
<https://doi.org/10.18297/etd/525>

This Master's Thesis is brought to you for free and open access by ThinkIR: The University of Louisville's Institutional Repository. It has been accepted for inclusion in Electronic Theses and Dissertations by an authorized administrator of ThinkIR: The University of Louisville's Institutional Repository. This title appears here courtesy of the author, who has retained all other copyrights. For more information, please contact thinkir@louisville.edu.

OPTIMIZATION OF PROCESS PARAMETERS FOR DIRECT METAL
DEPOSITION OF NICKEL

By

Steven James Gravatte
B.S., University of Louisville, 2004

A Thesis
Submitted to the
University of Louisville
J. B. Speed School of Engineering
as Partial Fulfillment of the requirements
for the Professional Degree

MASTER OF ENGINEERING

Department of Chemical Engineering

December 2005

OPTIMIZATION OF PROCESS PARAMETERS FOR DIRECT METAL
DEPOSITION OF NICKEL

By

Steven James Gravatte
B.S., University of Louisville, 2004

A Thesis Approved on

December 2, 2005

By the following Thesis Committee:

Thesis Director

ABSTRACT

This research was performed to establish the feasibility of using Direct Metal Deposition (DMD) technology to deposit nickel powder to a nickel substrate. The substrate is electrodeposited pure nickel, and the material to be deposited is Metco 56C-NS Nickel powder which is 99.5% nickel and 0.5% trace elements. The DMD process is a form of laser welding; metallic powder is fed into and melted by a high power CO₂ laser, which also melts the substrate. As the melted substrate and powder re-crystallize, they form a metallurgical bond, as opposed to the mechanical bond created in a normal welding process. The DMD equipment adds material to the substrate in layers; each previously added layer becomes the substrate for the subsequent layer. The process has a variety of parameters that affect the quality of the deposited material. Gas flow rates, laser power, and traverse rate are a few of the most important factors that affect the quality.

Historically nickel has been hard to weld; it tends to have significant porosity and cracking in the welded area. In industry this is corrected by adding a small amount of a different element. The element added depends on the nickel alloy that is being welded. In applications dealing with pure nickel, literature suggests that titanium be added to the weld filler to reduce the tendency to be porous and crack. The addition of titanium to nickel powder was evaluated in this research, since it is suggested to significantly improve the quality of the DMD process.

These experiments tested various levels of gas flow rates, laser power, traverse rate, and several levels of added titanium. These factors were evaluated to find which factors have the most significant affect on quality. The quality was determined by mechanical testing, visual inspection, and microstructure inspection. When the significant

factors where determined, values were found that gave the highest Rockwell hardness. These factors where evaluated to determine how similar the deposited material performed and matched the original nickel substrate.

From the results of the experiment, it is concluded that nickel powder can be deposited on a nickel substrate with a quality suitable of for industrial applications. The mechanical properties of the deposited nickel where lower than those of the original substrate, but the quality of the material was high. Subsequent processing, such as heat treatment, may be able to make the properties more similar. It was found that titanium was necessary for the deposition to be fully dense. Pure nickel was too porous to be used for industrial application.

It is recommended that more research be completed in finding how post processing would affect the properties of the welded material. Additional knowledge would be gained by using deposited nickel in an industrial application and finding if the difference in properties affects the process. Results from real world evaluation would determine where future research should be directed.

TABLE OF CONTENTS

APPROVAL PAGE.....	ii
ABSTRACT.....	iii
TABLE OF CONTENTS	v
LIST OF FIGURES	viii
I. INTRODUCTION.....	1
A. Overview.....	1
B. Literature Review.....	3
II. INSTRUMENTATION, EQUIPMENT AND MATERIALS	6
A. Direct Metal Deposition Machine (DMD 3000).....	6
B. Rockwell Hardness Tester	8
C. Instron 4505	9
D. Scanning Electron Microscope	9
E. Metallograph	10
F. Materials Preparation Equipment	11
G. Materials	11
III. PROCEDURE AND RESULTS.....	12
A. Preliminary.....	12
B. Initial Deposition: Elemental Nickel Metco 56C.....	13
C. DMD Parameters.....	17
D. Test Depositions	21
E. DMD with Alloying Elements Aluminum and Titanium.....	29
F. Experimental Analysis of Process Parameters.....	31

G. Statistical Analysis.....	37
H. Mechanical Testing.....	41
IV. CONCLUSIONS	46
V. RECOMMENDATIONS.....	47
LIST OF REFERENCES.....	48
APPENDIX I- Settings and Data from Experimental Testing	50
APPENDIX II-Minitab Output for Statistical Analysis	54
APPENDIX III-DMD Analog Settings vs. Real World Values.....	65
APPENDIX IV-Oxygen Test Results.....	67
APPENDIX VI-Recipes for All DMD Experiments	70

LIST OF TABLES

Table	Page
1. Typical DMD recipe values.....	18
2. Single line width and height measurements.	22
3. Hardness measurements from depositions on tooling substrate.	25
4. Factor Settings and Data for Runs 1-8.....	33
5. Factor Settings and Data for Runs 9-16.....	34
6. Factor Settings and Data for Runs 17-24.....	35
7. Possible Change in Hardness.....	39
8. Optimal Settings of Significant Parameters.....	40
9. Detailed results of Tensile Tests.....	45
10. Gage Reliability and Repeatability for the Rockwell Hardness Tester	67

LIST OF FIGURES

Figure	Page
1. DMD 3000	6
2. Nozzle Apparatus.....	7
3. Rockwell Hardness Tester	9
4. Dynazoom Metallograph	10
5. Baseline hardness measurements.....	13
6. Uneven deposition	14
7. Illustration of DMD overlap.	15
8. Typical DMD tool path.....	16
9. Single line test Samples.	22
10. Nickel test depositions.	23
11. Samples after hardness tests.	25
12. Metallography of nickel deposition.	26
13. DMD and TIG comparison.	26
14. DMD & TIG re-melting samples.....	27
15. DMD High vs. Low Reynolds number flow.	28
16. Hardness samples of alloyed and pure nickel depositions.....	29
17. Hardness indentions on Aluminum and Titanium alloyed samples.	30
18. Metallograph of Aluminum and Titanium alloyed samples.	30
19. Results from Runs 17- 24	36
20. Tensile bar cut from tool sample.	41
21. Tensile bar during machining 5% Ti	42

22. Tensile test results plot.	44
23. Powder Feed Rate Values.....	65
24. Values for Laser Power	66
25. Values for Gas Flow Rate.....	66

I. INTRODUCTION

A. Overview

This research was performed to determine operating parameters for the direct metal deposition (DMD) of nickel powder onto a nickel substrate. The automotive industry uses molds made of electrodeposited nickel for the production of vinyl dashboard skin. The common cause of failure in these tools is that cracks develop, allow steam from the steam jacket into the tool which makes bubbles form in the vinyl, ruining the vinyl skin. Currently the solution is to apply a temporary patch, silicone room temperature vulcanizing rubber, and to attempt to get continued service out of the tool. Some of the cracks in the nickel are large enough to eliminate the possibility of patching. Additionally, a crack repaired with a silicone patch continues to grow until the tool has to be repaired again, or taken out of service completely. The cost of these electrodeposited nickel tools is high and the temporary repair currently used is seen as inadequate, making a new repair method that permanently fixes cracks desirable.

Direct metal deposition has been used for a similar application, injection molding tool repair, and has the potential for use in repairing the nickel molds. The DMD process is described as near-net shape manufacturing, meaning that tools repaired in the DMD machine are oversized and need to have finishing work before being put into service. The DMD process uses a 3000 watt CO₂ laser to add metal powder to a metal substrate, by melting the substrate and the powder in the focal point of the laser. The mixture of melted powder and substrate cools quickly as the laser traverses

along, leaving a solid line of added material. This process is performed repeatedly, layer by layer, with the previously added material becoming the new substrate, until the final desired height defined by Computer Aided Design files is achieved.

Titanium, copper, and several steels have been used successfully in the process, all in applications where welding repairs were unsuitable or material costs made conventional manufacturing prohibitively expensive. The cost of the electrodeposited tools has provided a possible new application, if procedures for quality nickel depositions can be established. The large number of settings in the DMD process makes developing new settings a significant part of trying new materials. Settings such as laser power, traverse rate, and the various gas flow rates have to be evaluated at various settings to obtain quality deposition.

Nickel normally exists as a face-centered cubic crystal, but has been found in a hexagonal close packed in certain situations. Mild heating causes the hexagonal close packed structure to return to face centered cubic (Rosenberg, 1968). Since only one type of crystal structure is common, the properties of nickel are constant for most environments.

Nickel is resistant to atmospheric corrosion, and to a variety of corrosive agents. The automotive molds used in this project take advantage of this property. The mold must maintain a perfect surface finish and a high rate of heat transfer, and resist corrosion from the steam and vinyl slurry used in the process. Nickel has been reported to form a "superficial, tightly adherent scale" (Rosenberg, 1968, pg. 29). This thin oxide forms a protective layer on the surface of the metal and protects against other types of corrosion.

The focus of this project is to determine the operating parameters to produce depositions with properties similar to those of the electrodeposited nickel tool substrate.

B. Literature Review

Direct Metal Deposition and deposition manufacturing have been the topics of previous research in the last decade. Most of the research has involved Laser Engineered Net Shaping (LENS) technology sold by Optomec Inc., a technology similar to DMD. LENS systems use a neodymium-yttrium-aluminum-garnet (Nd-YAG) laser instead of the CO₂ laser used in the DMD system. The powder delivery system is also significantly different; LENS systems use four ports located 90° apart, while the DMD system is a concentric ring at the tip of the laser nozzle. These systems have been around for similar amounts of time, but the LENS system is smaller and less expensive than a DMD system. These differences have influenced more laboratories to choose LENS technology, which has resulted in more research on the LENS process. The processes are similar enough that parallels can be drawn from LENS studies to DMD technology.

Determining the effect of process parameters on the deposition was the specific topic of a paper by Kobryn, Moore, and Semiatin (2000). Their research involved determining the effects of laser power and traverse speed on the porosity and build height on Ti-6Al-4V samples. A LENS system was used to conduct the tests. The process parameters were varied according to a design of experiments. The microstructure, macrostructure, and build height of the samples were evaluated to determine the best operating parameters. Their results showed that porosity decreased at higher laser powers

and traverse speeds. Build height decreased when the traverse rate was increased, but the effects of laser power on deposition height were inconsistent.

Another article discusses the use of a custom built LENS-type machine for the deposition of nickel alloys (Peng, 2005). This research focuses on a relationship between specific energy and quality of the deposition. The quality was determined by examination of the deposition macrostructure and microstructure for porosity and cracking. The process parameters that were investigated were laser power, scan velocity, overlap, and powder feed rate. The goal of their project was to develop an overall term to predict deposition quality; this article suggests specific energy. The specific energy of the system is described by,

$$E = \frac{P}{DS} \quad (1)$$

where E is the specific energy, P is the laser power, D is the diameter of the spot size, and S is the scan velocity. Their experiment showed that direct laser fabrication can be used to deposit a nickel alloy, and that specific energy can be used to predict some characteristics of deposition quality. One of the conclusions of the article is that cracking and porosity are common defects in laser fabricated nickel depositions, a common problem mentioned for conventional welding of nickel and its alloys in the welding literature.

A study on the effects of variations in shaping gas flow (Fearon 2004) used maps of powder cloud geometry to determine ideal parameters for the deposition of 304L stainless steel. A camera was clamped near the end of the nozzle to study the shape of the flow of powder at different flow rates while building thin wall box structures. The results showed that the build height was highest when the particle cloud was smallest and the

particle velocity was low. Results of this article may not be identical to the same experiment repeated on a DMD system, but the effect of shaping gas on the build height is still relevant.

Several texts described porosity and cracking as a common problem when welding nickel. The same solutions to these problems are suggested in three different texts. Nickel and its Alloys, Welding and Brazing of Nickel and Nickel-Base Alloys, and The Metallurgy of Welding, Brazing, and Soldering, all suggest the addition of titanium to improve weld quality. This solution is prevalent throughout the welding community; according to American Welding Society classification ERNi-1, welding rods for high purity nickel projects have 93% min Ni, 2-3.5% Ti and small concentrations of several other elements.

II. INSTRUMENTATION, EQUIPMENT AND MATERIALS

A. Direct Metal Deposition Machine (DMD 3000)

A direct metal deposition machine is designed to bring together and house the components needed for the direct metal deposition process. These components include the Trumpf TLF 3000 Laser, the nozzle assembly, gas banks, a computer interface running proprietary software, and a significant amount of tubing and electrical wires.

The majority of the volume of the machine is the process chamber, which houses the nozzle and workspace for the process. Figure 1 shows a front view of the DMD machine, with the chamber doors open. The nozzle is visible in the center of the picture, as is the computer interface in front of the right door.

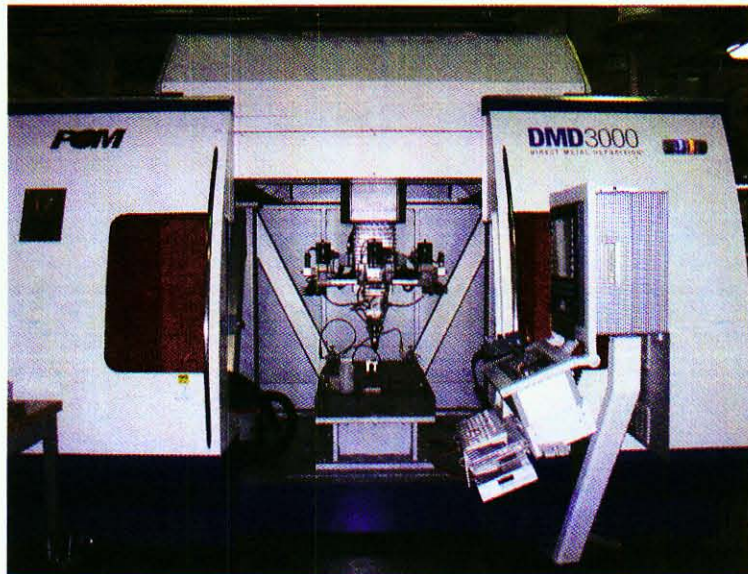


Figure 1. DMD 3000 Front View of Process Chamber

The nozzle assembly, shown in figure 2, is where the DMD process parameters are most significant. The nozzle is on the end of a gantry that moves the nozzle on three axes, x, y, and z.

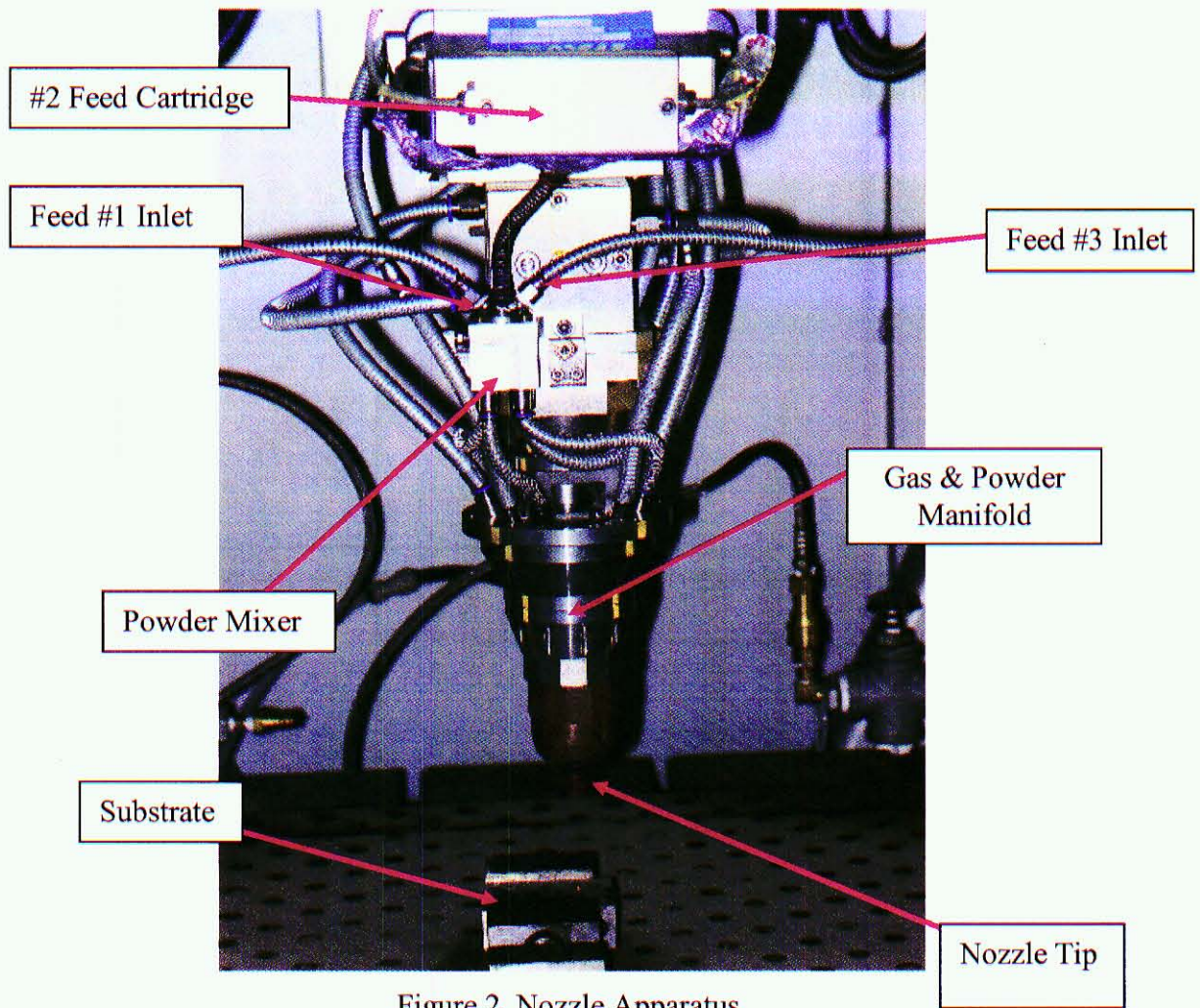


Figure 2. Nozzle Apparatus

Powder storage cartridges are located above the feed cartridges on three sides of the nozzle. These cartridges can be loaded with the same powder, or with different types of powders, and mixed in the process of injection into the laser beam. For this project, only one feed cartridge was used. The gases flow through tubing from tanks and bottles located behind the machine, into the nozzle manifold. The manifold routes the gases and powders to where they are delivered out of the nozzle tip. There are many small holes on the very tip of the nozzle where the gases and powder are delivered. The significant gases in this project are the shaping gas and the shielding gases. Argon is used as the shaping

gas, to make the powder and melted metal flow in the desired direction, and in combination with Helium as a shielding gas to prevent other, more reactive gases from contaminating the process.

The DMD machine is controlled by a computer interface that is fed instructions in the same way as a Computer Numerical Control (CNC) milling machine. Computer design files are used in a Computer Aided Manufacturing (CAM) software package for machining. These types of computer software output the desired toolpath into a code that is read by machining software attached to the mill, lathe, in this case, the DMD. The DMD 3000 uses proprietary software to control the “recipe” and uses the CAM data to operate the DMD process. Process parameters that can be changed constitute the “recipe” that is used in each deposition.

The Trumpf TLF, 3000-Watt, CO₂ laser is designed specifically for use in the DMD. High power output with a minimum penetration is desired in this process, as opposed to a moderate power, high penetration laser that would be used in laser cutting equipment.

B. Rockwell Hardness Tester

A Rockwell hardness tester, shown in figure 3, was used for measuring the hardness of the samples. These samples were measured in the Rockwell B scale with a silicon carbide sphere and a 100 kgf load. The difference in the penetration depth of a 10 kgf preload and the 100 kgf test load is the hardness of the material. The Rockwell B scale ranges from 0 to 100, with higher values corresponding to harder materials.



Figure 3. Rockwell Hardness Tester

C. Instron 4505

Tensile testing for the determination of physical properties of materials was completed using an Instron 4505 Universal Materials Testing Machine. This machine is capable of a wide variety of testing procedures including tension, compression, and flexure. Tensile tests were done on nickel rectangular specimens according to ASTM E 8 – 93: Standard Test Methods for Tension Testing of Metallic Materials.

D. Scanning Electron Microscope

A Jeol JSM- 5310 Scanning electron microscope with an EDAX Energy Dispersion Spectrometer (EDS) dewar-style attachment was used for the elemental analysis of metallic samples, and the examination of small cracks. The range of

magnification is 15x to 200,000x and it has a viewing diameter of 12.7 centimeters. The EDS attachment displays peaks based on x-ray emission from core electron energy levels, which are used to determine elemental composition.

E. Metallograph

Microstructures of metallic samples were analyzed with a Bausch & Lomb Dynazoom Metallograph, shown in figure 4. This metallograph has a magnification range of 80x to 400x and has a camera port to allow capture of images with any type of camera. This device was built in the early 1960's but was calibrated for this project.

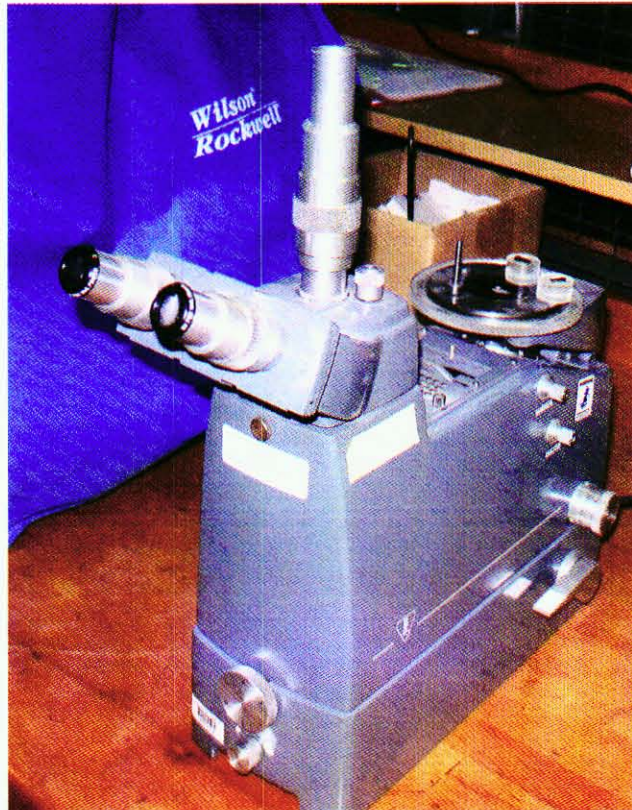


Figure 4. Dynazoom Metallograph

F. Materials Preparation Equipment

The metallic samples were specially prepared to view the microstructure.

Preparation started with cutting the sample into a usable size with the Isomet low speed saw. This saw uses a diamond cutting wheel to slowly cut this sample without causing the amount of heat generated with other types of saws. The sample is located on an arm above the wheel and has a variable amount of weight located on the top of the arm. A pool of cutting fluid is located below the wheel, allowing the bottom edge of the wheel to be immersed in the fluid.

Final preparations were made using an Ecomet 3 variable speed grinder- polisher. This polishing system uses an 8-inch wheel with interchangeable surfaces, which for this project ranged from 120 grit sandpaper to 1 micron diamond suspension on a cotton pad. The polishing wheel can be set to rotate from 0-500 rpm, and has a water jet for keeping the coarser grit paper cool and the grinding surfaces clean.

G. Materials

The material used is a commercially available plasma spray product produced by Sulzer Metco (Winterhur, Switzerland) under the brand name Metco 56C. The powder is supplied in the necessary -200 to +325 mesh size. Metco 56 C is 99.5% nickel with trace amounts of other elements. Pure titanium powder was purchased from Crucible Research (Pittsburg, PA) and was used as an additive in later parts of the research.

III. PROCEDURE AND RESULTS

A. Preliminary

Analysis of the project started with the examination of a failed tool obtained from a local automobile manufacturer. This mold supplied the material needed to perform the depositions and metallographic experiments for the project.

Nickel material samples from various sources were obtained and the hardness of each of these samples was measured and compared. A gage reliability & repeatability experiment was conducted for the Rockwell hardness tester to be used for all subsequent hardness measurements. The results of the gage reliability & repeatability are contained in Appendix III. Since hardness was to be used as a primary indicator of material quality for the DMD material, an understanding of the baseline hardness of the various nickel materials was needed. Nickel samples measured were:

1. Cut samples provided by the tool manufacturer, which represented nine different nickel tools
2. Sample obtained from the failed production tool
3. Nickel 200 , a 99.6% Nickel material purchased from a commercial supplier

Figure 5 is a comparison of the average hardness of the 11 baseline materials along with the approximate thickness of each.

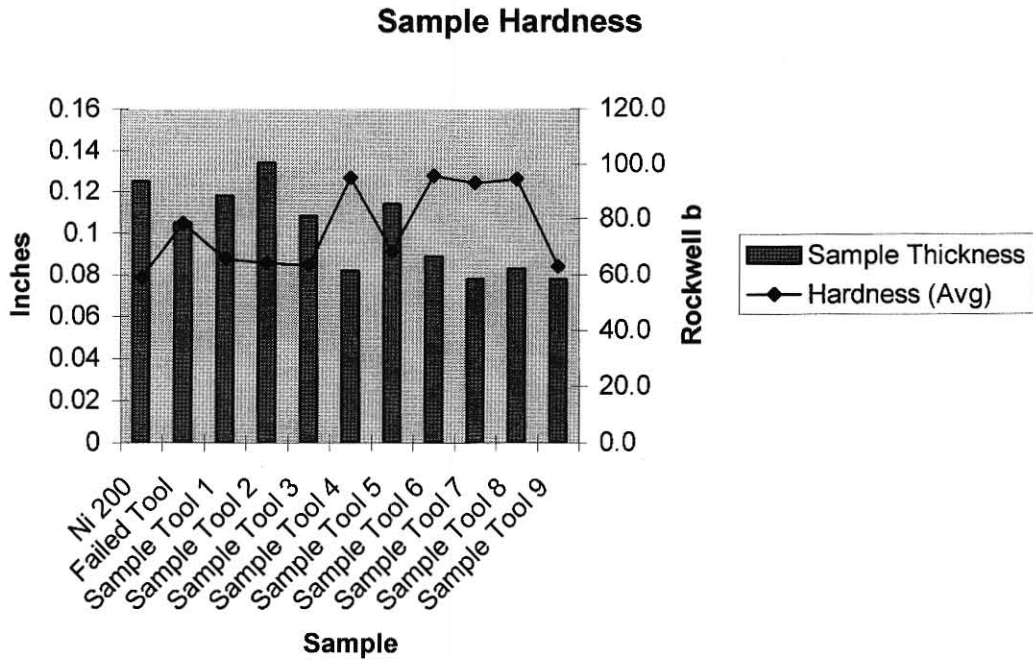


Figure 5. Baseline hardness measurements

The average hardness for the samples was 76.4 Rb, with a standard deviation of ± 15.13 . The variation in these readings is due to the variety in the measured samples. Since each sample was provided from the tool manufacturer, the variations in production, the location of the sample in the tool, and the level of use the tool received is unknown. The variation in these numbers illustrates the differences in hardness in tools from the manufacturer, and provides a target for hardness values in the DMD samples later in experimentation.

B. Initial Deposition: Elemental Nickel Metco 56C

The first step in beginning DMD of a new material is to characterize the deposit geometry at various power levels. These data are required in order to construct an accurate tool path with correct step over, overlap, and inter-layer offset height.

The geometry of the laser deposited material can vary when starting with a cold substrate, and several layers are typically measured in order to average the effects of thermal changes over time. At the start of the deposition cycle on a “cold” substrate the deposition has a greater height and width at the beginning of a weld line. As the surrounding atmosphere, substrate, and deposition temperatures continue to rise the build height decreases, as can be seen in Figure 6. The height of the deposited material decreases in height from the start of the deposition (left) to the end of the deposition (right).

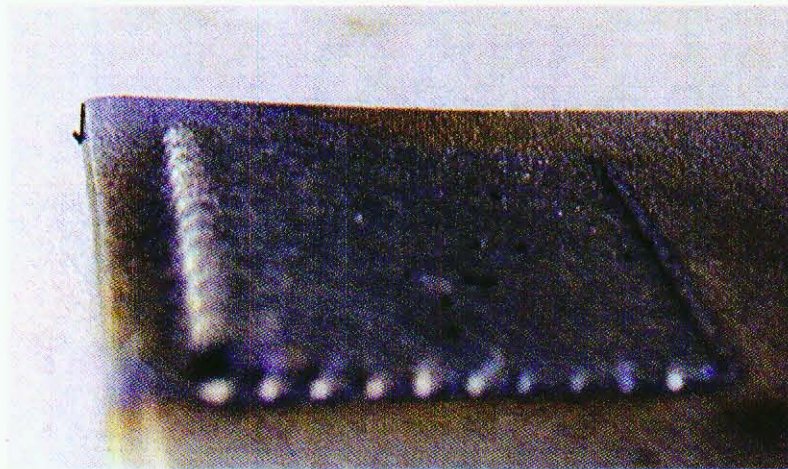


Figure 6. Uneven deposition

If the mass of the work piece is large then a quasi-steady-state temperature is reached where the heat radiated from the work piece is equivalent to the heat input by the laser energy. If the mass and/or area of the work piece is not large enough then the temperature will continue to rise during the deposition process. Uncontrolled temperature rise can negatively affect the deposition and usually results in an uneven build height and porous and cracked material.

The width of one deposition line is measured in order to program the correct offset between passes of the weld bead. Each pass overlaps the previous pass by

approximately 30%. Since the weld bead is assumed hemispherical in shape, the 30% overlap or 70% offset, results in a scalloped surface appearance. The amount of overlap has been optimized experimentally by the POM Corporation, developers of the DMD technology. The image shown in Figure 7 represents the overlapping nature of the deposited material.

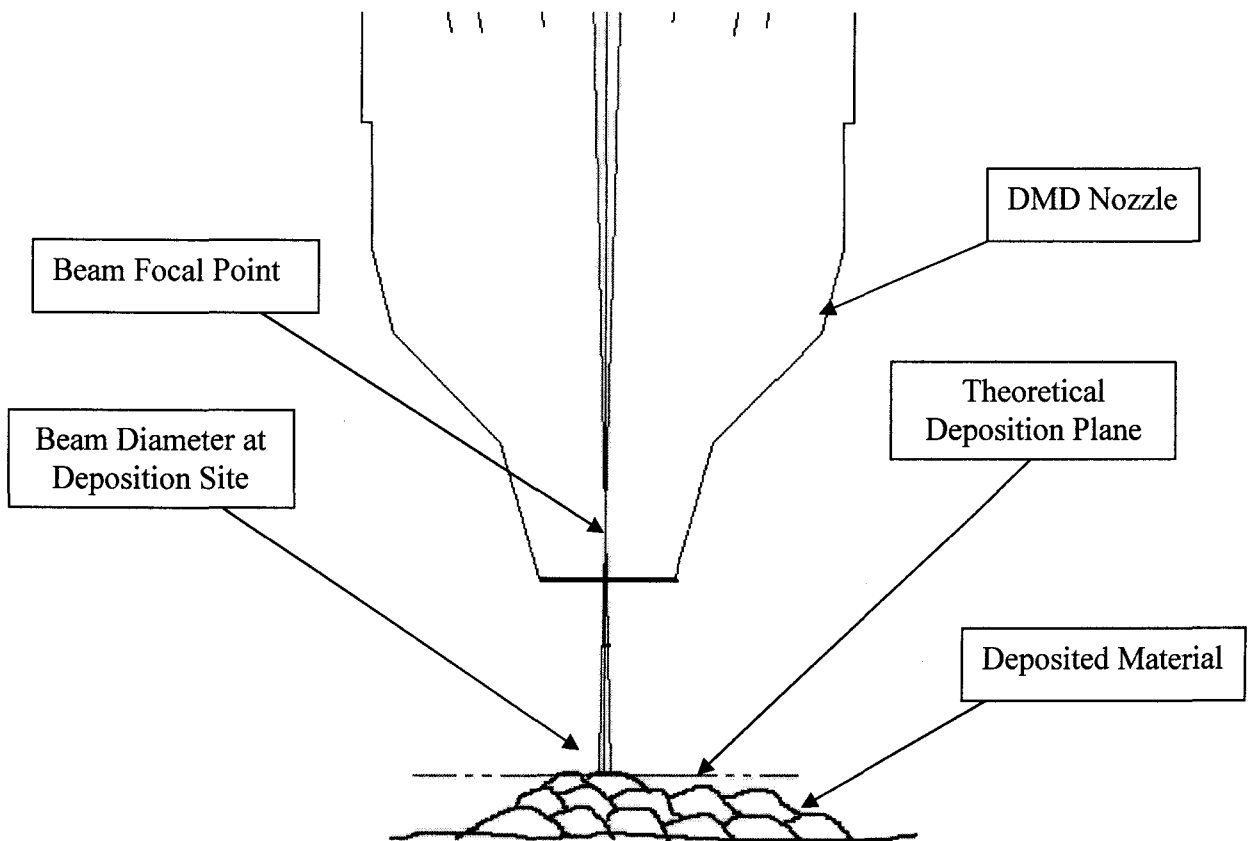


Figure 7. Illustration of DMD overlap.

This 30% value gives a uniform surface height while still allowing an economical amount of material deposition. Overlap values that are too small result in a “speed bump” scalloped surface, and lack of fusion between layers, while too large of an overlap will result in build height error propagation and lack of fusion to the substrate. Multiple layers consisting of the 30% overlap raster lines are typically required to complete a metal deposition for most applications. The amount of offset height between layers is

determined experimentally by depositing a known number of layers and averaging each build height per layer by measuring the total build height. Figure 8 shows a computer representation of a typical DMD path. Note the direction of travel for each deposition layer is orthogonal to the previous layer. This technique helps minimize height errors and also helps reduce the warping effects of thermal stresses.

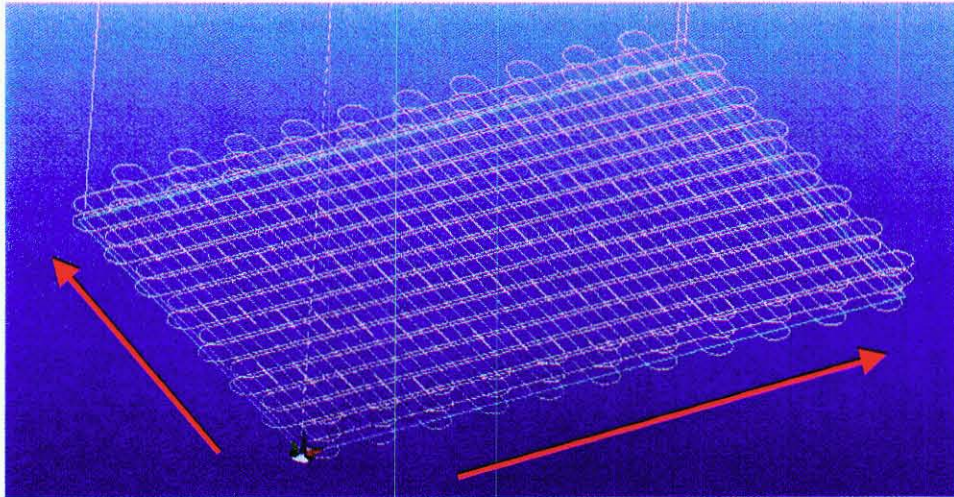


Figure 8. Typical DMD tool path.

Small variations in build height per layer are common and several techniques are employed to minimize variation and error propagation. Depositions with small volume and a relatively small total build height (less than .05" for instance) usually are not susceptible to height error problems. However care must be taken in all cases to minimize this error as it can affect consistency of the layer height and material quality. Build height error propagation occurs when the programmed height offset between layers is more or less than the actual build height of the deposition. As the build progresses, each successive layer ends further from the focal point of the laser beam. This results in uncontrollable variations in power density that can have negative effects on deposition quality.

C. DMD Parameters

The parameters that control the DMD process are stored in a table format referred to as a “recipe”. Recipe values are loaded into the DMD computer at the beginning of each laser deposition cycle and contain important process parameter data to control such variables as Gas Flow Rate, Laser Power, Traverse Rate, and Mass Flow Rate. All control variable values are set by an integer in the range 0 to 2000 with the exception of the laser frequency value, which is a hexadecimal number. The integer must be calibrated at the machine to correspond to a measured value. A typical recipe is shown in Table 1 with numbered rows corresponding to each recipe entry. An explanation of each recipe entry follows.

Table 1. Typical DMD recipe values.

	Parameter	Set Point
1	Shaping gas flow Ar	1000
2	Cover gas flow Ar	100
3	Carrier Flow Ar	200
4	Carrier Flow He	50
5	Nozzle Gas Flow Ar	1000
6	Nozzle Gas Flow He	100
7	Hopper Rate	100
8	Measured Rate	4.85
9	Control Laser Power	1400
10	LCD Laser Power	2130
11	Laser Freq	1280
12	CNC Vel (in/min)	20

Each recipe is identified and referenced inside the CNC program by the recipe I.D. number. Multiple recipes are stored for use with different material and substrate combinations.

1. Shaping gas flow is a pure argon stream that exits the nozzle at the bottom coaxial to the powder flow. The shaping gas flows through a series of angled laminar flow channels. The purpose of the shaping gas is to focus the powder exiting the nozzle by pushing it into a conical shape aimed at the area where melting occurs, thereby increasing the yield of the DMD process.
2. Cover gas flows into the powder feed cartridge and acts as a make-up gas, preventing a negative pressure inside the powder feed cartridge. It also acts as a

positive pressure purge of inert gas, limiting the raw powder exposure to the atmosphere. Cover gas flow rate is very small and remains fixed for all DMD processes.

3. Carrier gas assists the powder flow through the delivery system from the powder feed cartridge and through the nozzle manifold to the nozzle exit. It is a mixture of argon and helium, where parameter 3 is the value for argon in the mixture. Flow rate of carrier gas is typically fixed and small changes to carrier gas flow rate produce no measurable change in the DMD process. The percentage of argon in the mixture is the set point value for argon divided by the sum of the set point values of both argon and helium.
4. Flow rate of helium in the carrier gas mixture.
5. Nozzle gas acts as the main shielding gas for the welding process and is fed through the center of the nozzle coaxial to the laser beam. Nozzle gas is a mixture of argon and helium that shields the molten metal from atmospheric contamination. The percentage of argon in the mixture is the set point value for argon divided by the sum of the set point values of both argon and helium. Parameter 5 is the flow rate of argon in the nozzle gas. Nozzle gas flow rate has a considerable effect on deposited material quality. Gas flow rate calibration charts are contained in appendix II.
6. Flow rate of helium in the nozzle gas mixture.
7. The hopper rate refers to the speed of the mechanical motor incorporated into each powder feed cartridge. The hopper rate directly correlates to the mass flow rate of material into the weld pool. Mass flow rate must be calibrated for each

new material by measuring the mass flow of material per unit time thru the DMD nozzle. The DMD 3000 has a specific routine for testing powder flow rate of each hopper during a 2-minute test cycle. Charts for material flow rate calibration are contained in appendix II.

8. Measured rate is the mass flow rate of powdered metal through the nozzle and is measured and reported by the DMD Machine. The flow rate corresponds to the programmed hopper rate value in recipe entry 7.
9. Laser Power refers to the amount of energy output by the laser resonator. Control values range from 0 to 2000 and correspond roughly to values of 0 to 3150 watts of laser power at the resonator. It has been found that the laser beam loses approximately 10% of its power thru reflection and transmission losses inside the beam delivery tubes. Laser power is calibrated using the built-in power meter on the laser power supply cabinet which measures the laser power inside the resonant chamber.
10. LCD laser power is the reading on the laser power supply cabinet which measures the laser power inside the resonant chamber. Charts for laser power calibration are contained in appendix II.
11. Laser Frequency is a hexadecimal number that corresponds to a frequency range at the laser power supply of approximately 100 to 10,000 hz. The setting 1280 in the DMD recipe corresponds to 5Khz laser frequency. All testing for this project was conducted at this frequency, since all previous work was performed at this setting.

12. CNC Velocity controls the linear speed at which the laser beam traverses across the substrate. Deposition velocity is a very important variable affecting the quality of deposited material. Velocity affects the heating, residence, and cooling times for the molten material.

D. Test Depositions

The first step in test deposition for new material as described above is to deposit a single line and measure the deposited width and height of the line. Sixteen runs were conducted, some of which are shown in Figure 9, with results shown in the Table 2. The runs varied in scan speed and laser power as shown, while all other parameters are set to standard values from Table 1. Runs 1 through 3 and runs 1a through 3a did not deposit a measurable amount of material. The material used for these tests was Metco 56C, and the substrate material was 0.125" Nickel 200 sheet. Table 2 shows the measured values of the line widths and heights, along with Specific Energy in N/m.

Specific energy has been suggested as a method to predict deposition quality. In these samples several runs had similar specific energies, 1 was similar to 3a, 2 to 5a, and 3 to 7a. These tests yielded insufficient data to examine specific energy, since runs 1, 2, and 3 deposited too little powder to judge the quality.

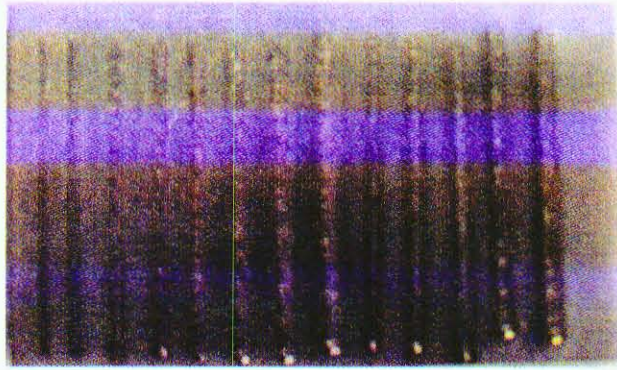


Figure 9. Single line test Samples.

Table 2. Single line width and height measurements.

Run #	Rate ipm	Watts	Width	Height	Specific Energy
1	10	640	n/a	n/a	1.16E+09
2	10	966	n/a	n/a	1.76E+09
3	10	1280	n/a	n/a	2.33E+09
4	10	1600	0.03	0.004	2.91E+09
5	10	1915	0.04	0.007	3.48E+09
6	10	2215	0.05	0.008	4.03E+09
7	10	2500	0.055	0.009	4.54E+09
8	10	2833	0.06	0.009	5.15E+09
1a	20	640	n/a	n/a	5.82E+08
2a	20	966	n/a	n/a	8.78E+08
3a	20	1280	n/a	n/a	1.16E+09
4a	20	1600	0.03	0.004	1.45E+09
5a	20	1915	0.04	0.004	1.74E+09
6a	20	2215	0.05	0.005	2.01E+09
7a	20	2500	0.055	0.006	2.27E+09
8a	20	2833	0.06	0.007	2.57E+09

Once the line width and heights were determined, programs were written with the appropriate offset values in order to establish a starting point for the deposition of the nickel material. The 10 successful single line trial data were programmed into 10 separate test geometries.

Test depositions were conducted using the Nickel 200 alloy as a substrate. The first test depositions were 0.75 square inches in area, 1" by 0.75", and 5 layers deep. The heat input to the substrate for the first few depositions indicated that the total heat input

was too high for this experiment. Significant melting and distortion of the substrate occurred. The area of deposition was reduced by one half in order to reduce the net heat input to the substrate.

A test sample consisting of ten, 0.375 square inch, 0.5" by 0.75", depositions was created using data obtained from the 10 successful single line tests. Each deposition was conducted at the power level and traverse rate shown in Table 2, as well as having a CNC program tailored for each separate deposition geometry. Once the parameters for successful deposition can be narrowed, a single deposition geometry can be used. Figure 10 below shows the finished test plate.

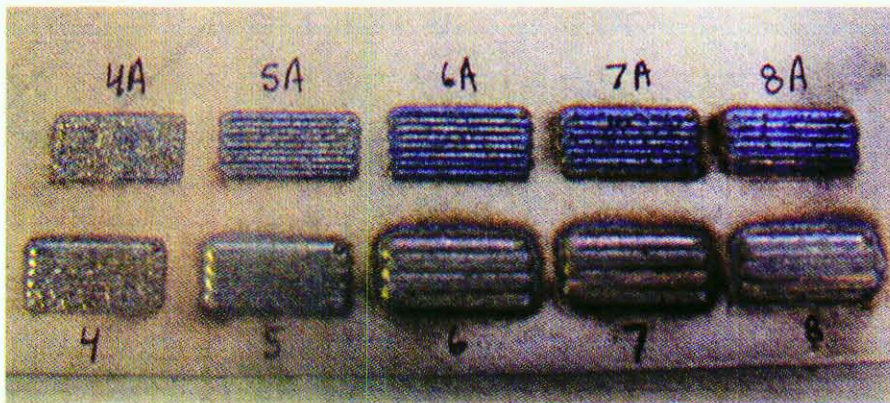


Figure 10. Nickel test depositions.

Run numbers 4 through 8, conducted at lower traverse rates, showed obvious porosity and uneven build height, which is normally a sign of excessive heating. Optimization of the DMD parameters begins from a set point established by visual inspection of the deposition geometry. The key elements to observe are a uniform bead width and overlap, uniform build height, and minimal heating of the substrate. Visible indications of poor weld quality include obvious porosity or voids, lack of fusion, cracking, and insufficient overlap. A low power optical microscope is used to aid in

determining deposit quality at the initial stage. Based on the results of the initial set point trial, recipe parameters that correspond to the values near those of runs 6A and 7A were chosen for the next set of experiments. These samples displayed less porosity, no surface cracks, and even build height.

Deposition widths of 0.05” and a build height of 0.011” were assumed and a new deposition program was written. The new-programmed build geometry was 0.5” by 0.75” with 5 layer height and a 5 second pause between each layer. The pause is included in the program to allow heat to dissipate before adding another layer. The test substrate was also allowed to cool to room temperature between depositions to eliminate the cumulative effect of heating the substrate during each deposition.

The next step in optimizing the deposition parameters was to add hardness measurements of the samples in addition to the visual indicators. Hardness has been shown to be a key parameter in identifying DMD deposit quality. In a quality deposition, there are no visible defects, and the hardness of the deposition is similar to the hardness of the substrate. Consistently low hardness numbers can be an indication of porosity. Large variation in hardness across a sample can indicate voids or lack of fusion.

Setting from 10 of the 16 runs on the Ni200 substrate were duplicated on electrodeposited tool substrates and hardness values for all runs were measured with disappointing results. Runs 1-3 and 1a-3a were not used since those settings produced negligible build height in the initial test. After machining the samples obvious porosity was found in more than half the depositions. The hardness values for all depositions were extremely low, indicating a consistent porosity problem. Table 3 shows low and inconsistent hardness values for nearly all test runs. Values of zero are the result of the

sample being so soft that the hardness testing equipment could not report a value in the Rockwell b range.

Table 3. Hardness measurements from depositions on tooling substrate.

Run #	Hardness Values			Average	Std. Dev.
4	54	22	0	25.3	27.2
5	35	27	20	27.3	7.5
6	0	0	0	0.0	0.0
7	0	0	0	0.0	0.0
8	0	0	0	0.0	0.0
4a	57	61	56	58.0	2.6
5a	57	60	58	58.3	1.5
6a	61	62	61	61.3	0.6
7a	44	43	50	45.7	3.8
8a	24	17	14	18.3	5.1

Figure 11 shows the test samples after machining and measuring for hardness. Note the obvious porosity and the depth of indentation of the hardness test sites compared with the substrate, which tested at 85.2 ± 2.4 Rb.

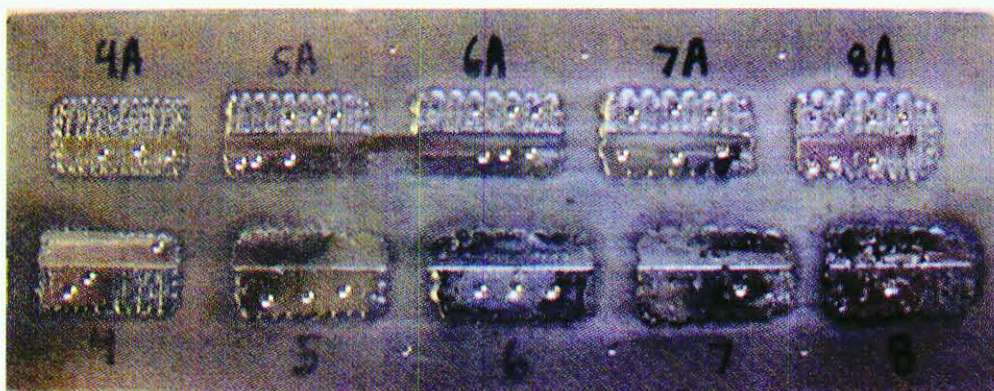


Figure 11. Samples after hardness tests.

The target hardness for the depositions was near that of the substrate, approximately 80 Rb. However the best hardness achieved was a full 25% below the target hardness at run 6a parameters. The presence of significant porosity was confirmed by metallography. An extensive test of 25 more parameter combinations was conducted

in an effort to eliminate the porosity problem with no gain in deposition quality. Figure 12 shows typical metallograph images of the porous material.

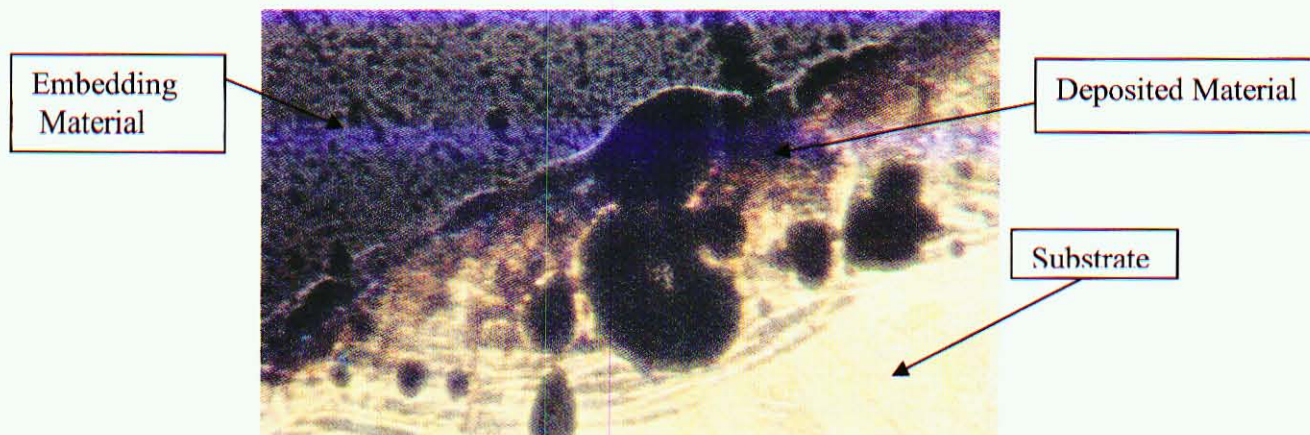


Figure 12. Metallography of nickel deposition.

Several approaches were utilized in an effort to isolate the source of the porosity. Typical adjustments to the DMD parameters had failed to produce a porosity free weld; nickel depositions with DMD were porous and crack filled. A similar process, Tungsten inert gas (TIG) welding was tried on several samples using Nickel 200 as a filler metal. TIG welding produced acceptable quality welds, but because the energy from the TIG welder is less precise than the DMD, it produces a larger heat affected zone. Figure 13 shows two metallographic images of TIG and DMD produced welds with obvious quality differences.

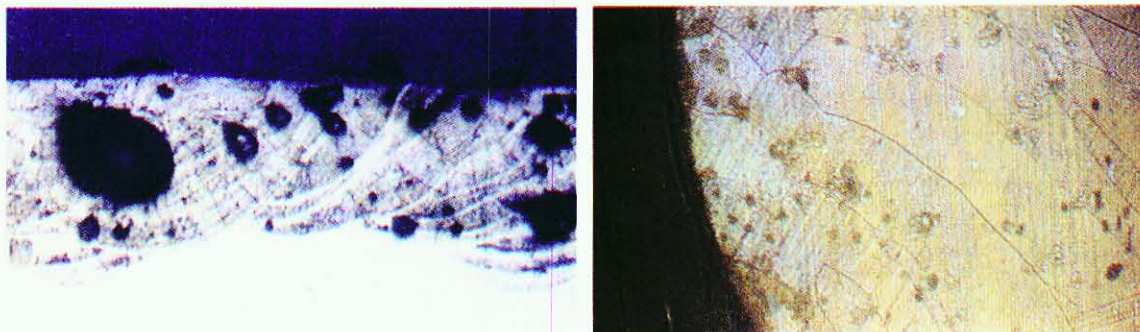


Figure 13. DMD and TIG comparison.

Since TIG welding was able to produce a nonporous weld, the differences between DMD and TIG were each considered as a possible source of the porosity.

1. Energy Source
2. Filler Metal
3. Shielding Gas

Experiments were conducted in order to isolate the source of the porosity.

Substrate material was subjected to thermal energy from both the laser beam and the TIG torch without the addition of the filler metal. By operating the processes without filler material, it was shown that the DMD process creates the porosity, not the nickel powder.

Figure 14 below shows the comparison of laser melted nickel and TIG melted nickel.

There is obvious porosity evident in the DMD melted nickel sample.

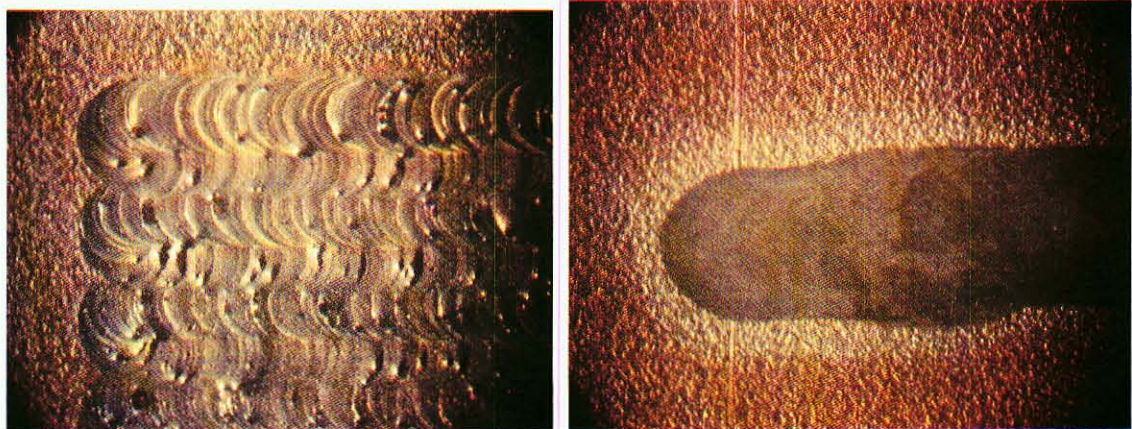


Figure 14. DMD & TIG re-melting samples.

The only remaining parameter that could be changed was the shielding gas flow rate. Using the TIG flow rate of 15 to 30 cubic feet per hour, an approximate flow rate for the DMD was calculated to be 7 to 14 lpm. The gas flow rate used in the DMD process had been 35-40 lpm. The Reynolds number for the high gas flow rate is 1680, a value which is near the transition range for a circular pipe, which is 1800-2300. The lower

range for gas flow rate gives a Reynolds number of 470, indicative of laminar flow and a value well below the transition stage. These are crude estimates since the flow area is not fully developed in a long tube. This flow rate was then applied to the nozzle gas flow of the DMD machine and the experiment was repeated. The result was a dramatic improvement in weld quality as seen in Figure 15.

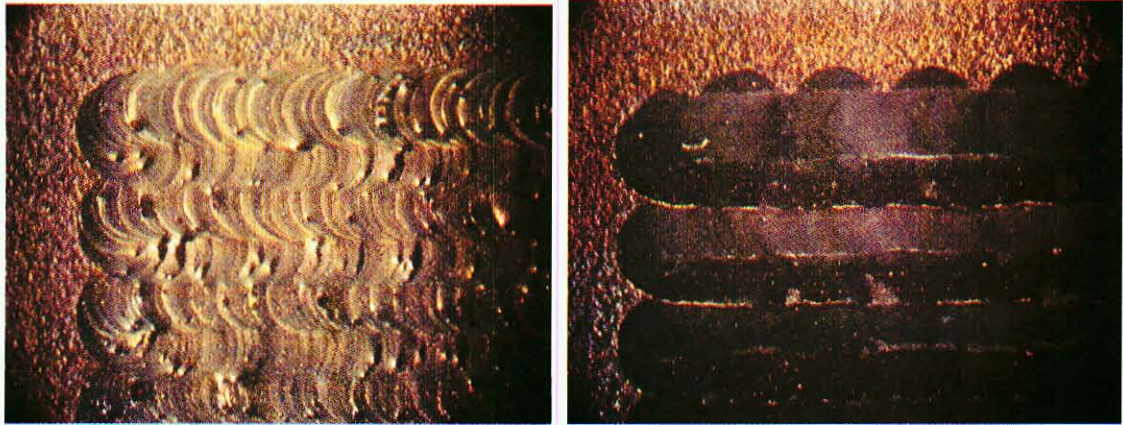


Figure 15. DMD High vs. Low Reynolds number flow.

Now that a major quality factor had been identified, the original tests were duplicated to see if good quality nickel depositions could be obtained.

Visual quality of the depositions under the new gas flow parameters was superior to any previous deposition; however the material hardness was still greatly reduced. This indicated the material was still porous and not fully dense. Modifying the gas flow rate reduced the size of the porosity and eliminated surface cracking on the depositions.

After conducting over 30 test depositions it was determined that the best hardness that could be obtained was approximately 20% below the desired hardness. The deposited material still contained micro porosity that was affecting the material hardness and quality. In order to conduct a design of experiments, a reliable measure of material

quality was needed. Until the porosity issues could be sorted out, any data from a design of experiments would be unusable.

Research and welding techniques suggest that the solution to the porosity issue lay in the chemical composition of nickel and nickel alloy wires for MIG and TIG welding. American Welding Society classification ERNi-1 nickel welding wire contains 2.0 to 3.5% titanium, and up to 1% aluminum, as well as other trace elements.

E. DMD with Alloying Elements Aluminum and Titanium

Experiments were prepared to deposit new nickel material containing various concentrations of aluminum and titanium. Detailed process parameters and recipe values for all depositions are located in Appendix V.

Figure 16 shows the effects of adding 3% titanium and 3% aluminum by weight. The hardness of the alloyed depositions was increased dramatically.

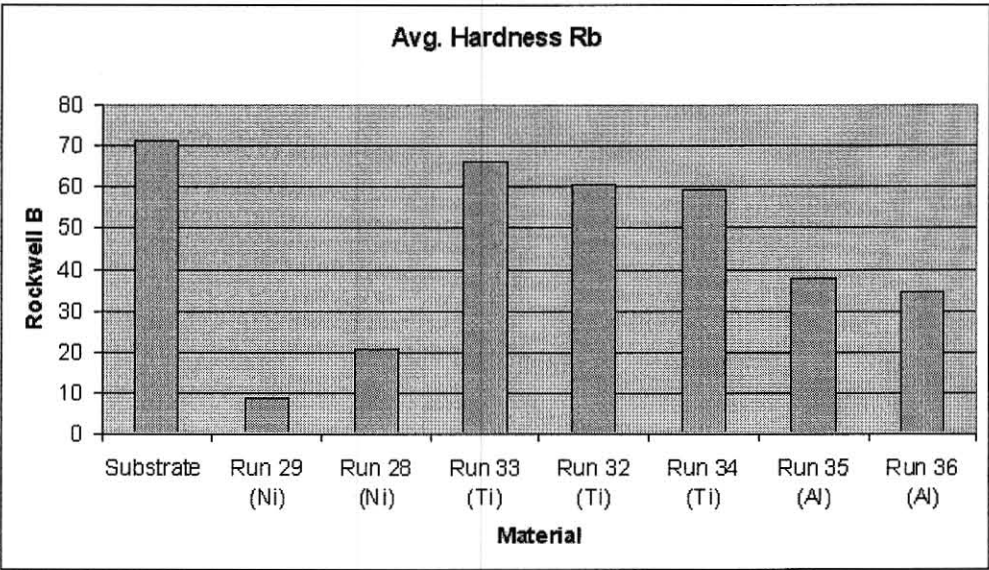


Figure 16. Hardness samples of alloyed and pure nickel depositions.

The addition of aluminum increased deposition hardness, but not to the substrate value. Figure 17 at left shows stress cracks forming around the Rockwell indentations of the aluminum-alloyed samples, while the figure at right shows the higher integrity of the titanium-alloyed deposition.

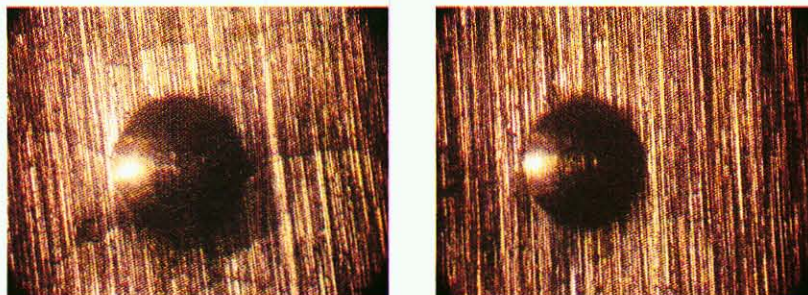


Figure 17. Hardness indentations on Aluminum and Titanium alloyed samples.

Metallography of the nickel, aluminum-alloyed, and titanium-alloyed samples correlate with the hardness data. The addition of aluminum reduced porosity but did not eliminate it. The titanium additions however produced high hardness samples with no porosity. Figure 18, left, shows the aluminum-alloyed deposition, and right, the titanium-alloyed deposition.

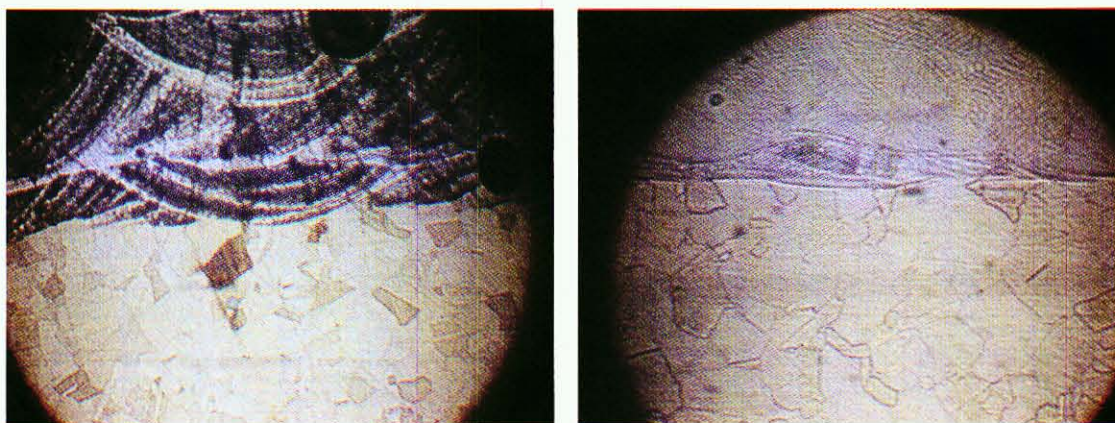


Figure 18. Metallograph of Aluminum and Titanium alloyed samples.

An outside lab was contacted to perform oxygen analysis on several representative samples, in an attempt to better understand why the addition of titanium improves the quality of the deposition. Combustion–infrared absorbance, according to ASTM 1019-03, was performed by IMR Test Labs in Ithaca, NY. Four samples were submitted for testing, a piece of the failed tool, a sample of deposited pure nickel, a sample of deposited Ni with 3% Ti, and a sample of Metco 56 C nickel powder. The results of this test are shown in Appendix IV. The addition of the titanium reduced the oxygen in the deposited sample to less than one third of that in the pure nickel deposition and about half of what was in the nickel powder. This may be a problem with the test method, caused by the titanium reacting with the oxygen in the test system. Combustion-infrared absorbance measures CO and CO₂ in the gases exiting the sample chamber when the sample and a graphite sample are heated. If the oxygen reacts with the titanium, the measurements would be inaccurate, since only oxygen in CO₂ is measured. The electrodeposited nickel tool has very low oxygen content due to the production method. With fully dense material and a reliable method to evaluate samples with the hardness tester, a formal design of experiments could now be performed.

F. Experimental Analysis of Process Parameters

Experiments were conducted for the evaluation of the effect of process parameters on the hardness of deposited nickel samples. The experiments involved the variation of the parameters over a range of values in the normal operating range. Deposited samples were machined and tested for hardness. The samples were evaluated based on the results of the hardness testing.

The factors for this experiment are gas flow rate, laser power, concentration of titanium added to the nickel powder, and traverse rate of the nozzle across the substrate. The gas flow rate is a combination of the amount of shaping and nozzle gas used in the deposition process. The shaping gas controls the shape of the powder cone feed into the laser, and the nozzle gas shields the deposition from atmospheric contamination. The levels for gas flow rate were 11 liters per minute and 35 liters per minute, which represent the range for normal operation of the DMD machine. The levels of laser power were 1850 watts and 2450 watts, which are 15% higher and lower than the operating range for steel, and would be considered the “normal” operating range. The levels for concentration of titanium additive, 3% and 5% titanium added, are based on values from welding rod standards. Traverse rate levels, 15 and 20 inches per minute, is the range for normal DMD operation.

The response variable is Rockwell hardness, which is a quick and simply performed test that allows for comparative analysis. Electrodeposited nickel, the substrate of this project, has a hardness of around 70-80 Rockwell B scale. The deposited material should have a similar hardness, when deposited on this substrate. Since initial testing has shown that the hardness of the depositions has been less than that of the substrate, the goal is to maximize deposition hardness. The samples are machined flat, and tested at five points across the surface.

The first eight experiments were completed on a nickel substrate, while holding traverse rate at 20 inches per minute. Other factors were varied as shown on Table 4, along with the data from the hardness testing.

Table 4. Factor Settings and Data for Runs 1-8

Run Order	Gas Flow Rate (Liters/Minute)	Laser Power (Watts)	Concentration of Ti (%)	Average Hardness (Rockwell B)	Standard Deviation(+/-)
1	11	1850	3	67.4	2.30
2	35	1850	3	70.4	1.56
3	11	2450	3	68.4	0.42
4	35	2450	3	67.7	1.20
5	11	1850	5	74.8	1.04
6	35	1850	5	75.8	2.46
7	11	2450	5	75	2.15
8	35	2450	5	75	1.06

During DMD operation, experimental runs with low gas flow rates were observed to be running very hot, especially when combined with a high laser power as in runs 3 and 7. These settings were judged to be too hot for safe operation and the ranges were modified for subsequent runs. The new settings for gas flow rate were 17 and 40 liters per minute, the same size range as the first eight runs, but increased to lower the heat in the deposition. Levels of laser power for subsequent runs were also changed to 1570 watts and 2166 watts, again to have the same range as before, but to lower the heat in the system.

It was also evident that the concentration of titanium had a significant impact on the hardness. All depositions at 5% titanium added were significantly harder than those at 3% titanium. Since this parameter had such an evident effect, and material expenses are high, this factor was held at 5% for the remainder of the experiment. A new factor traverse rate, evaluated over range of 15 to 20 inches per minute replaced titanium concentration in subsequent tests.

Eight more samples were deposited on a nickel substrate and were damaged in processing. Pieces of the electrodeposited nickel tool were being used as the substrate for

experimentation. Processing the samples on these sections of the tool was difficult for several reasons, primarily because of problems in machining the finished depositions flat. The sections of the tool are thin and hard to fixture in a machining process. A steel bar was used as a substrate in subsequent runs to eliminate these difficulties in the processing stage. This had an affect on the hardness values, but with statistical analysis this effect can be quantified and the effect of other factors can still be determined.

The experimental conditions that led to damaged samples were repeated on a steel bar substrate. These experiments used nickel with 5% titanium and variations in other factors as shown in Table 5 along with the data.

Table 5. Factor Settings and Data for Runs 9-16

Run Order	Gas Flow Rate (Liters/Minute)	Laser Power (Watts)	Traverse Rate (Inches/Minute)	Average Hardness (Rockwell B)	Standard Dev. (+/-)
9	17	1570	15	86.4	0.82
10	40	1570	15	84.2	1.15
11	17	2166	15	85.2	1.10
12	40	2166	15	83.4	1.47
13	17	1570	20	86	0.71
14	40	1570	20	84	1.41
15	17	2166	20	85	1.22
16	40	2166	20	83.6	0.89

Hardness is an easy test that allows for easily comparable results, but other factors can be considered in defining optimal settings. One such factor is resulting build height of the deposition, which has a large impact on the cost of the DMD process. Metal powders are expensive, and it has been shown in other studies (Davis, 2004), that gas flow rate can have a pronounced effect on build height.

The next experiments were designed to test the effect of variations in gas flow rate on the deposition height when using nickel in the DMD process. Eight samples were

run varying the gas flow rate from 10 lpm to 66 lpm in increments of eight lpm. This covers the full extent of the DMD machine's operational range. The other process parameters were held constant at a laser power of 1850 watts, a traverse speed of 20 inches per minute, and a titanium concentration of 5%.

Samples of 0.5" by 0.75" and five layers thick were deposited on a steel bar, to allow for easy measurements and testing. When the samples finished and cooled, the overall height of each sample was measured. They were then ground flat and tested for hardness. The run settings and results are shown in Table 6.

Table 6. Factor Settings and Data for Runs 17-24

Sample #	Gas Flow (Lpm)	Deposition Height	Hardness (Rockwell B)	Standard Dev. Of Hardness (+/-)
17	10	0.032	85.6	1.14
18	18	0.032	87.6	1.14
19	26	0.034	86.6	1.14
20	34	0.028	86.4	1.14
21	42	0.029	86.4	0.55
22	50	0.023	82.6	1.14
23	58	0.022	79.2	1.64
24	66	0.019	77.4	1.35

The data show higher build heights at a gas flow rates of 10-26 lpm, and the highest hardness values at flow rates of 10-18 lpm. Deposition height shows a larger range, and has a more pronounced decrease after the peak value. When these data are displayed graphically, as in Figure 19, the group of flow rates with the highest hardness and build heights can be seen relative to the lower hardness and heights at higher flow rates.

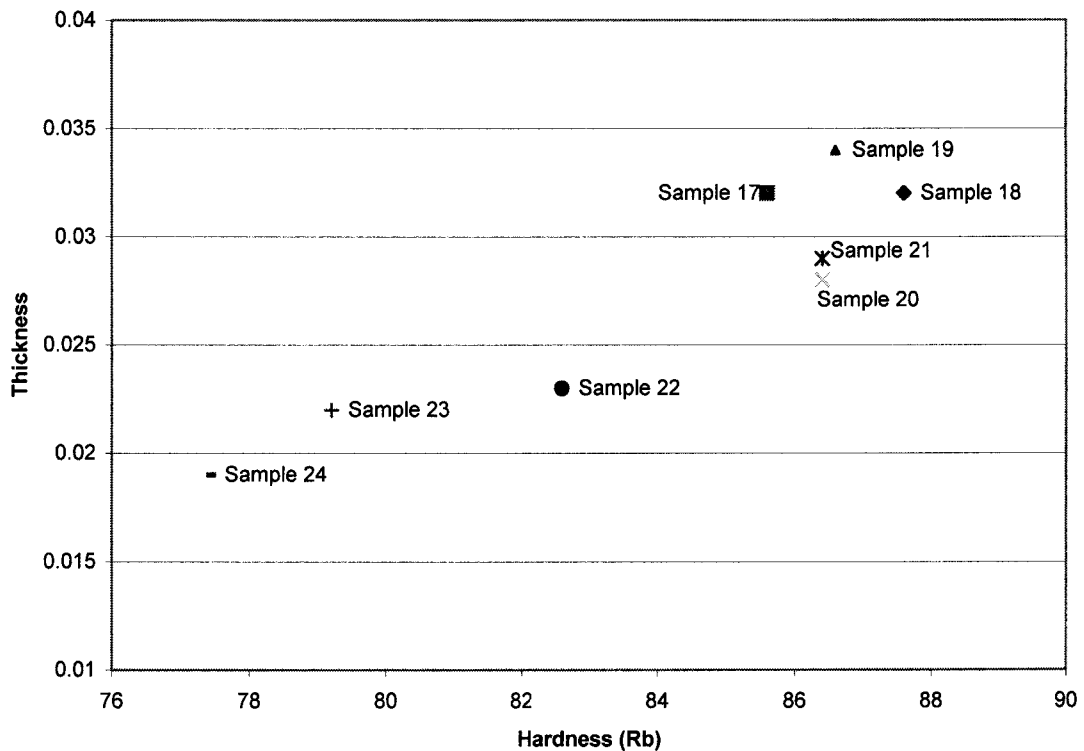


Figure 19 Results from Runs 17- 24

The results of these eight experiments show that hardness and build height are maximized at gas flow rates around 18-26 lpm. Operation in this range provides high hardness values and allows for more cost effective depositions. This shows how pronounced the effect of gas flow rate is on the properties of the deposition.

Deposition height is a function of the amount of powder that is fed, and how much is actually deposited. The powder efficiency, in this case based on build height, is the percentage of the feed material that goes into the actual deposition and, is important for several reasons. If the powder efficiency is low, the project will take longer, since more layers must be made to reach the final height. This results in more material used, and more time out of production for the tool being repaired.

G. Statistical Analysis

Data from the experiments were analyzed using Minitab statistical analysis software. Variations in factor levels, and the number of factors in the 24 experiments limited the types of analysis that could be performed. Since the goal is to maximize the response variable, hardness, regression was determined to be the most fitting form of statistical analysis. Finding a regression model, and using the model to maximize hardness would determine the optimum settings for the operating parameters.

All hardness value measurements from the 24 experiments were entered into the software, along with the settings for each run. All data and settings used in this analysis are found in Appendix I. Minitab's regression function was used to find a regression model based on all factors, hardness, gas flow rate, laser power, concentration of titanium, substrate and all interactions of the factors. The Minitab output for this and all analysis in this section of the project can be found in Appendix II.

The terms in this model were evaluated for relevancy based on their probability values (p-values). Probability values can be used to evaluate the significance of a statistical term. In the statistical analysis, if a factor is assumed to have no effect on a population, the p-value will show if this hypothesis is true or false. If the hypothesis is true, the population is not effected by the factor; the p-value will be near 1. If the hypothesis is false, the population is effected by the factor; the p-values will be close to zero, meaning the term is statistically significant.

The model showed that most of the interactions terms were not significant. To simplify and provide a more realistic model, interaction terms with low significance,

based on their p values, were eliminated. Experimental factors were left in the model regardless of p-value since these contribute to the interactions and must be considered as part of the model. A new regression model was developed in Minitab and interaction terms were judged for significance based on p-values. Terms with low significance were removed and the process repeated.

When all interaction terms involving traverse rate were eliminated, this term was removed as well. The p-values for this term were consistently among the highest in the analysis, meaning the value for traverse rate is statistically insignificant. New models were created and terms eliminated until a model was found that had terms with p-values lower than 0.05, a normal standard for determining significance. This model is shown below,

$$H = 68.4 - 0.299 * G - 0.00387 * P + 3.34 * T + 9.94 * S + 0.000106 * G * P \quad (2)$$

where H is hardness, G is gas flow rate, P is laser power, T is the concentration of titanium, S is the substrate. Substrate is based on values of 0, if the substrate is nickel, and 1, if the substrate is steel. All other terms are in the units used throughout the experiments.

The adjusted R^2 value for this model is .909. Adjusted R^2 is a measure of how well the model fits the data that also considers the number of model parameters and number of data points used in the analysis. The value represents how much of the data could be predicted by the model. Models with higher R^2 values fit the data better than models with lower R^2 values. This model fits almost 91% of the data, which is considered a good fit.

The settings of the process parameters can be optimized with this model using the coefficients and range of settings for each term. If the coefficient is positive than the value should be maximized, if negative, the parameter should be set to its minimum. The changes in hardness can be seen in Table 7.

Table 7. Possible Change in Hardness

Factor	Factor Setting	Affect on Hardness	Possible Δ Hardness
Substrate (Steel=1, Nickel=0)	1	9.94	9.94
	0	0	
Titanium Concentration (%)	3	10.02	6.68
	5	16.7	
Gas Flow Rate (lpm)	17	-0.5083	0.6877
	40	-1.196	
Laser Power (W)	1570	-6.0759	2.30652
	2166	-8.38242	
Gas/Laser Interaction	low	2.82914	6.3547
	high	9.18384	

The choice of substrate has the highest possible affect on hardness. Since the term is positive, it should be maximized to have a positive impact on the deposition hardness. Since the settings for substrate are either 0 for nickel or 1 for steel, it is determined that the depositions on steel substrates yield the highest hardness values. This is to be expected since the steel substrate has a higher hardness than the nickel substrate, and the hardness tester measures the hardness of both the deposition and the substrate at the point of testing. In practical situations this parameter would not be set by the operator, but by the project.

Concentration of titanium in the feed material has the next highest possible affect on hardness. The coefficient is positive, meaning this value should be maximized. Since

five percent is the highest concentration used in testing, and the highest shown for use in high purity welding, this is determined to be the optimal setting.

Laser power and gas flow rate have an interaction term that is considered in the model. The possible affect on the hardness must be considered since the interaction term coefficient is positive and the coefficients of laser power and gas flow rate are negative. Since the possible affect on hardness is greater for the interaction, the values of the parameters with must be optimized based on the interaction term, rather than the individual factors. Since the interaction term is positive, the values for gas flow rate and laser power should be maximized.

The optimal value for laser power is the highest values in the range, which was determined to be 2166 watts. A higher value, such as 2450 watts used in four of the first eight experiments, would produce harder depositions, but was determined to be unsafe for normal operation. Gas flow rate should also be operated at the highest possible setting in the experimental range, but as shown in the last eight experiments, it can also have a large effect on resultant build height. Since the effect on the hardness is minimal relative to that of the concentration, and the effect on build height so pronounced, the optimum setting was determined to be 26 lpm. The optimal values for significant parameters that can be set by the operator are shown below in Table 8.

Table 8. Optimal Settings of Significant Parameters

Factor	Gas Flow Rate (Liters/Minute)	Laser Power (Watts)	Concentration of Titanium
Optimal Setting	26	2166	5%

H. Mechanical Testing

Baseline mechanical properties for the electrodeposited nickel were established by machining 3 tensile bars from tool samples. Figure 20 shows a typical tensile bar after testing.

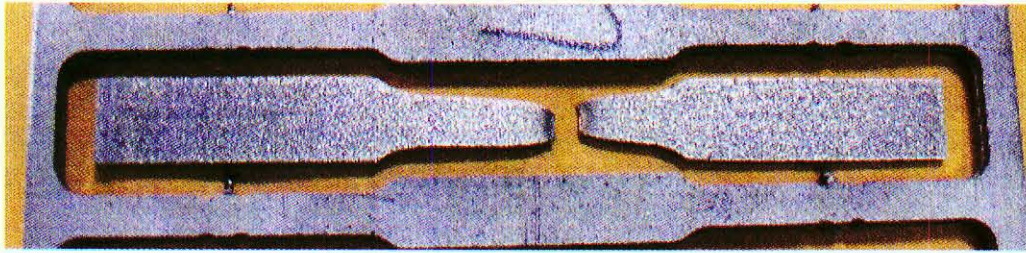


Figure 20. Tensile bar cut from tool sample.

A method for creating a DMD tensile bar from the titanium-alloyed material was needed. Based on the hardness data that showed the 5% titanium-alloyed DMD samples to have the highest hardness, an initial tensile bar was fabricated from this material. The first tensile sample was created by depositing a thick section (approx. 0.150") onto a steel substrate. The tensile bar shape was then machined and removed from the steel substrate. This method did produce a useable tensile bar but was very challenging and time-consuming. Figure 21 shows a successful tensile bar near completion machined, from a solid DMD 5% titanium-alloyed deposition.

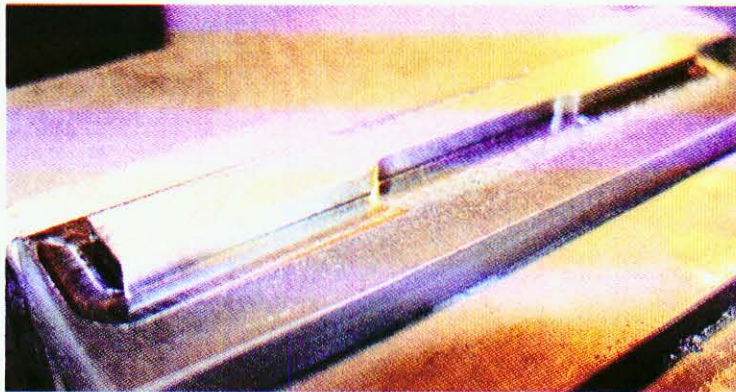


Figure 21. Tensile bar during machining 5% Ti

The challenge in producing a tensile bar is that the substrate material tends to warp significantly when a large bulk of DMD material is deposited. In order to control the warping, a very thick substrate with a large thermal mass is needed. This complicates the machining and removal of the tensile bar after the DMD is completed. The deposition of such a large amount of material is also complicated by the accumulation of thermal stresses in the tensile bar sample. Precautions must be taken to minimize the total heat input during the deposition in order to minimize thermal stress and distortion that can cause cracking in larger sample volumes. A solution was developed to diminish these issues.

By depositing a DMD tensile bar onto a square tubing substrate, most of the benefits of a solid substrate could be realized while allowing for easier removal of the tensile bar from the substrate. This method did not eliminate the problems, but did speed up the processing time and allow for the creation of more tensile bars.

The tensile testing was conducted first on the baseline tensile bars cut from the tooling material. The next bar to be tested was the 5% titanium-alloyed DMD sample. The results of the tensile test showed a significant reduction in plastic deformation as compared to the baseline sample. To determine if the concentration of titanium was

responsible for the loss of ductility, three tensile bars were fabricated from 3% titanium-alloyed nickel. The combined results of all seven tensile tests are shown in Figure 22 and Table 9. The 5% titanium-alloyed DMD sample actually had the highest strength of any of the DMD tensile samples. The 3% titanium-alloyed samples showed no increase in ductility and yielded at a much lower stress value than the 5% sample. Since there was improvement in mechanical properties gained by using the 3% titanium alloy, and the 5% titanium-alloy produced harder samples, 5% was determined to be the optimal setting.

Stress - Strain Nickel Baseline & DMD Tensile Bars

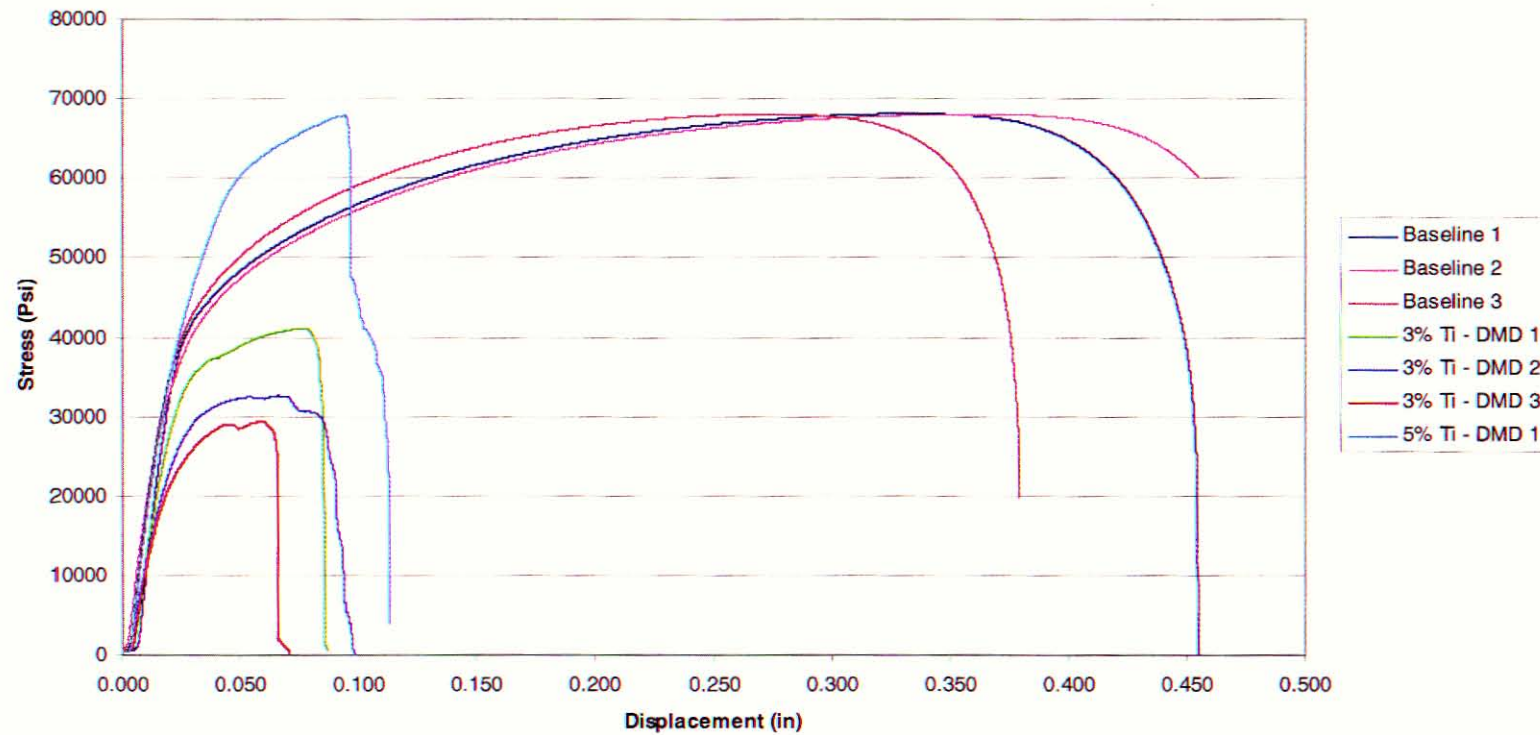


Figure 22. Tensile test results plot.

Table 9. Detailed results of Tensile Tests.

Sample	Strain Peak (%)	Load at Peak (lbf)	Stress Peak (psi)	Disp. at Break (in)	Strain Break (%)	Load at Break (lbf)	%Elong @Break
Substrate 1	22	1868	68195	0.4540	30.3	623	29.72
Substrate 2	24	1838	68112	0.4900	32.7	530	32.12
Substrate 3	18	1424	68101	0.3790	25.3	532	24.64
3%Nickel DMD 4	5	1268	41142	0.0850	5.7	874	4.74
3%Nickel DMD 5	4	995	32628	0.0970	6.5	83	6.36
3%Nickel DMD 6	4	891	29366	0.0650	4.3	723	3.45
5%Nickel DMD 7	6	1944	67972	0.1130	7.5	556	6.98
	Stress Break (psi)	Disp at 0.2% (in)	% Strain at 0.2%	Load at 0.2% Yield (lbf)	Stress at 0.2%	Energy at Yield (lbf-in)	Energy at Break (lbf-in)
Substrate 1	22737	0.0241	1.606	1038	37890	10.92	731.67
Substrate 2	19641	0.0207	1.383	899	33311	10.06	782.72
Substrate 3	25438	0.0214	1.428	756	36154	8.06	467.23
3%Nickel DMD 4	28358	0.0224	1.493	915	29699	9.33	83.06
3%Nickel DMD 5	2706	0.0203	1.353	702	23016	6.89	73.99
3%Nickel DMD 6	23829	0.0190	1.270	613	20220	5.41	43.31
5%Nickel DMD 7	19430	0.0242	1.611	1130	39511	13.38	156.49

IV. CONCLUSIONS

- DMD Process parameters were optimized within the testing range based on deposition thickness and material hardness. The highest quality depositions corresponding to the highest process yield occurred with laser power, velocity, and gas flow rates of 2166 watts, 20 inches per minute, and 26 liters per minute respectively.
- The primary source of poor weld quality was determined to be turbulent flow of shielding gas. By reducing the combined gas flow rates of the nozzle gasses below the transition zone, porosity was greatly reduced.
- Porosity could not be completely eliminated without the addition of small amounts of alloying elements. Additions of elemental titanium in concentrations of 3% and 5% by weight eliminated porosity and increased hardness in the nickel DMD deposits.
- DMD Tensile bars made with nickel-titanium alloy showed large variations in yield strength and lower ductility than the substrate material. DMD tensile bars also showed very little plastic deformation compared to the substrate material.

V. RECOMMENDATIONS

- EDAX or other elemental composition study of alloyed DMD samples to confirm titanium concentration levels.
- Investigate causes of low ductility of DMD tensile bars, such as residual stresses caused by thick depositions, or by iron migration from substrate material.
- Conduct investigation of laser annealing and substrate pre-heating techniques and their effect on deposition hardness and ductility. Investigate methods to deposit a more ductile material with the addition of alloying elements.

LIST OF REFERENCES

- Davis, T. 2004. The Effect of Process Parameters on Laser Deposited Ti-6Al-4V. M. Eng. Thesis, University of Louisville.
- Fearon, E. and Watkins, K. 2004. Optimization of Layer Height Control in Direct Laser Deposition. 23rd International Congress on Applications of Laser & Electro-optics paper No. 1708.
- Fessler, J., Merz, R., Nickel, A., and Prinz, F. 1996. Laser Deposition of Metals for Shape Deposition Manufacturing. Solid Freeform Fabrication Proceedings 117-124.
- Fessler, J., Nickel, A., Link, G., and Prinz, F. 1997. Functional Gradient Metallic Prototypes through Shape Depositions Manufacturing. Solid Freeform Fabrication Proceedings 521-528.
- Gabe, D. R., Principles of Metal Surface Treatment and Protection. New York: Pergamon Press Inc., 1972
- Kobryn, P. A., More, E. H., and Semiatin, S. L. 2000. The Effect of Laser Power and Traverse Speed on Microstructure, Porosity, and Build Height in Laser-Deposited TI-6AL-4V Scripta Materialia 43:299-305.
- Lancaster, J. F. The Metallurgy of Welding, Brazing, and Soldering. New York: American Elsevier Publishing Company Inc., 1965
- Mankins, W. L., Nickel Alloys Huntington Alloys International Technical Bulletin 1-17
- Montgomery, D. C. 2005. Design and Analysis of Experiments New Jersey: John Wiley and Sons
- Mortland, J. E., Evans, R. M., and Monroe, R. E., Welding and Brazing of Nickel and Nickel-Base Alloys. Washington, D. C.: National Aeronautics and Space Administration: Technology Utilization Office. 1972.
- Nickel, A., Barnett, D., Prinz, F. 2001. Thermal Stresses and Deposition Patterns in Layered Manufacturing Materials Science and Engineering A317:59-64.
- Noecker, F. F. and Dupont, J. N. 2002. Functionally Graded Copper – Steel Using Laser Engineered Net Shaping Process. Solid Freeform Fabrication Proceedings 231-238.

Peng, L., Taiping, Y., Sheng, L., Dongsheng, L. Qianwu, H., Weihao, X., and Xiaoyan, Z. 2005. Direct Laser Fabrication of Nickel Alloy Samples Internaitonal Journal of Machine Tools and Manufacture 45:1288-1294

Rosenberg, S. J., Nickel and Its Alloys. Washington, D. C.: National Bureau of Standards: Institute for Materials Research. 1968

Ross, R. B., Handbook of Metal Treatments and Testing. New York: John Wiley and Sons, Inc., 1977

Thomas, A. 2004. Fabrication of Ti-6Al-4V Structures Using Direct Metal Deposition (DMD) Process. M. S. Thesis, University of Louisville.

Thornton, E. and Baker, W. A. D. 1962. Viscosity and Thermal Conductivity of Binary Gas Mixture: Argon-Neon, Argon-Helium, and Neon-Helium Proc. Phys. Soc. 80:11711175.

Vicars, J. 2005. Private communication.

APPENDIX I

Settings and Data from Experimental Testing

Run #	Gas Flow Rate	Laser Power	Conc. Of Ti	Traverse Rate	Substrate	Hardness	BC	BD	CD	BE	CE	DE	BF	CF	DF	EF	BCD	BCE	BDE	CDE	BCF	BDF	CDF	BEF	CEF	DEF	BCDE	BCDF	BCEF	BDEF	CDEF	BCDEF
1-1	10	1850	3	20	0	67	18500	30	5550	200	37000	60	0	0	0	0	55500	370000	600	111000	0	0	0	0	0	0	1110000	0	0	0	0	0
1-1	10	1850	3	20	0	67	18500	30	5550	200	37000	60	0	0	0	0	55500	370000	600	111000	0	0	0	0	0	0	1110000	0	0	0	0	0
1-1	10	1850	3	20	0	69	18500	30	5550	200	37000	60	0	0	0	0	55500	370000	600	111000	0	0	0	0	0	0	1110000	0	0	0	0	0
1-1	10	1850	3	20	0	70	18500	30	5550	200	37000	60	0	0	0	0	55500	370000	600	111000	0	0	0	0	0	0	1110000	0	0	0	0	0
1-1	10	1850	3	20	0	64	18500	30	5550	200	37000	60	0	0	0	0	55500	370000	600	111000	0	0	0	0	0	0	1110000	0	0	0	0	0
1-2	34	1850	3	20	0	68	62900	102	5550	680	37000	60	0	0	0	0	188700	1258000	2040	111000	0	0	0	0	0	0	3774000	0	0	0	0	0
1-2	34	1850	3	20	0	72	62900	102	5550	680	37000	60	0	0	0	0	188700	1258000	2040	111000	0	0	0	0	0	0	3774000	0	0	0	0	0
1-2	34	1850	3	20	0	71.5	62900	102	5550	680	37000	60	0	0	0	0	188700	1258000	2040	111000	0	0	0	0	0	0	3774000	0	0	0	0	0
1-2	34	1850	3	20	0	70.5	62900	102	5550	680	37000	60	0	0	0	0	188700	1258000	2040	111000	0	0	0	0	0	0	3774000	0	0	0	0	0
1-2	34	1850	3	20	0	70	62900	102	5550	680	37000	60	0	0	0	0	188700	1258000	2040	111000	0	0	0	0	0	0	3774000	0	0	0	0	0
1-3	10	2450	3	20	0	68.5	24500	30	7350	200	49000	60	0	0	0	0	73500	490000	600	147000	0	0	0	0	0	0	1470000	0	0	0	0	0
1-3	10	2450	3	20	0	68.5	24500	30	7350	200	49000	60	0	0	0	0	73500	490000	600	147000	0	0	0	0	0	0	1470000	0	0	0	0	0
1-3	10	2450	3	20	0	68	24500	30	7350	200	49000	60	0	0	0	0	73500	490000	600	147000	0	0	0	0	0	0	1470000	0	0	0	0	0
1-3	10	2450	3	20	0	68	24500	30	7350	200	49000	60	0	0	0	0	73500	490000	600	147000	0	0	0	0	0	0	1470000	0	0	0	0	0
1-3	10	2450	3	20	0	69	24500	30	7350	200	49000	60	0	0	0	0	73500	490000	600	147000	0	0	0	0	0	0	1470000	0	0	0	0	0
1-4	34	2450	3	20	0	66	83300	102	7350	680	49000	60	0	0	0	0	249900	1666000	2040	147000	0	0	0	0	0	0	4998000	0	0	0	0	0
1-4	34	2450	3	20	0	68.5	83300	102	7350	680	49000	60	0	0	0	0	249900	1666000	2040	147000	0	0	0	0	0	0	4998000	0	0	0	0	0
1-4	34	2450	3	20	0	69	83300	102	7350	680	49000	60	0	0	0	0	249900	1666000	2040	147000	0	0	0	0	0	0	4998000	0	0	0	0	0
1-4	34	2450	3	20	0	67	83300	102	7350	680	49000	60	0	0	0	0	249900	1666000	2040	147000	0	0	0	0	0	0	4998000	0	0	0	0	0
1-4	34	2450	3	20	0	68	83300	102	7350	680	49000	60	0	0	0	0	249900	1666000	2040	147000	0	0	0	0	0	0	4998000	0	0	0	0	0
1-5	10	1850	5	20	0	74	18500	50	9250	200	37000	100	0	0	0	0	92500	370000	1000	185000	0	0	0	0	0	0	1850000	0	0	0	0	0
1-5	10	1850	5	20	0	75	18500	50	9250	200	37000	100	0	0	0	0	92500	370000	1000	185000	0	0	0	0	0	0	1850000	0	0	0	0	0
1-5	10	1850	5	20	0	76.5	18500	50	9250	200	37000	100	0	0	0	0	92500	370000	1000	185000	0	0	0	0	0	0	1850000	0	0	0	0	0
1-5	10	1850	5	20	0	74.5	18500	50	9250	200	37000	100	0	0	0	0	92500	370000	1000	185000	0	0	0	0	0	0	1850000	0	0	0	0	0
1-5	10	1850	5	20	0	74	18500	50	9250	200	37000	100	0	0	0	0	92500	370000	1000	185000	0	0	0	0	0	0	1850000	0	0	0	0	0
1-6	34	1850	5	20	0	72	62900	170	9250	680	37000	100	0	0	0	0	314500	1258000	3400	185000	0	0	0	0	0	0	6290000	0	0	0	0	0
1-6	34	1850	5	20	0	77	62900	170	9250	680	37000	100	0	0	0	0	314500	1258000	3400	185000	0	0	0	0	0	0	6290000	0	0	0	0	0
1-6	34	1850	5	20	0	75	62900	170	9250	680	37000	100	0	0	0	0	314500	1258000	3400	185000	0	0	0	0	0	0	6290000	0	0	0	0	0
1-6	34	1850	5	20	0	76.5	62900	170	9250	680	37000	100	0	0	0	0	314500	1258000	3400	185000	0	0	0	0	0	0	6290000	0	0	0	0	0
1-6	34	1850	5	20	0	78.5	62900	170	9250	680	37000	100	0	0	0	0	314500	1258000	3400	185000	0	0	0	0	0	0	6290000	0	0	0	0	0
1-7	10	2450	5	20	0	77.5	24500	50	12250	200	49000	100	0	0	0	0	122500	490000	1000	245000	0	0	0	0	0	0	2450000	0	0	0	0	0
1-7	10	2450	5	20	0	74	24500	50	12250	200	49000	100	0	0	0	0	122500	490000	1000	245000	0	0	0	0	0	0	2450000	0	0	0	0	0
1-7	10	2450	5	20	0	76.5	24500	50	12250	200	49000	100	0	0	0	0	122500	490000	1000	245000	0	0	0	0	0	0	2450000	0	0	0	0	0
1-7	10	2450	5	20	0	75	24500	50	12250	200	49000	100	0	0	0	0	122500	490000	1000	245000	0	0	0	0	0	0	2450000	0	0	0	0	0
1-7	10	2450	5	20	0	72	24500	50	12250	200	49000	100	0	0	0	0	122500	490000	1000	245000	0	0	0	0	0	0	2450000	0	0	0	0	0
1-8	34	2450	5	20	0	74	83300	170	12250	680	49000	100	0	0	0	0	416500	1666000	3400	245000	0	0	0	0	0	0	8330000	0	0	0	0	0
1-8	34	2450	5	20	0	75.5	83300	170	12250	680	49000	100	0	0	0	0	416500	1666000	3400	245000	0	0	0	0	0	0	8330000	0	0	0	0	0
1-8	34	2450	5	20	0	76.5	83300	170	12250	680	49000	100	0	0	0	0	416500	1666000	3400	245000	0	0	0	0	0	0	8330000	0	0	0	0	0
1-8	34	2450	5	20	0	74	83300	170	12250	680	49000	100	0	0	0	0	416500	1666000	3400	245000	0	0	0	0	0	0	8330000	0	0	0	0	0
1-8	34	2450	5	20	0	75	83300	170	12250	680	49000	100	0	0	0	0	416500	1666000	3400	245000	0	0	0	0	0	0	8330000	0	0	0	0	0

APPENDIX II

Minitab Output for Statistical Analysis

Regression Analysis: Hardness versus Gas Flow Rate, Laser Power, ...

* DE is highly correlated with other X variables
* DE has been removed from the equation.
* DF is highly correlated with other X variables
* DF has been removed from the equation.
* EF is highly correlated with other X variables
* EF has been removed from the equation.
* BDE is highly correlated with other X variables
* BDE has been removed from the equation.
* CDE is highly correlated with other X variables
* CDE has been removed from the equation.
* BDF is highly correlated with other X variables
* BDF has been removed from the equation.
* CDF is highly correlated with other X variables
* CDF has been removed from the equation.
* BEF is highly correlated with other X variables
* BEF has been removed from the equation.
* CEF is highly correlated with other X variables
* CEF has been removed from the equation.
* DEF is highly correlated with other X variables
* DEF has been removed from the equation.
* BCDE is highly correlated with other X variables
* BCDE has been removed from the equation.
* BCDF is highly correlated with other X variables
* BCDF has been removed from the equation.
* BCEF is highly correlated with other X variables
* BCEF has been removed from the equation.
* BDEF is highly correlated with other X variables
* BDEF has been removed from the equation.
* CDEF is highly correlated with other X variables
* CDEF has been removed from the equation.
* BCDEF is highly correlated with other X variables
* BCDEF has been removed from the equation.

The regression equation is

Hardness = 26.8 + 1.67 Gas Flow Rate + 0.0106 Laser Power + 7.08 Conc.
Of Ti
+ 0.51 Traverse Rate + 22.1 Substrate - 0.000651 BC - 0.215
BD
- 0.00160 CD - 0.0212 BE - 0.00008 CE - 0.418 BF - 0.00393
CF
+ 0.000094 BCD + 0.000006 BCE + 0.000127 BCF

Predictor	Coef	SE Coef	T	P
Constant	26.76	41.94	0.64	0.525
Gas Flow Rate	1.669	1.423	1.17	0.243
Laser Power	0.01062	0.02185	0.49	0.628
Conc. Of Ti	7.084	4.276	1.66	0.101

Traverse Rate	0.515	1.903	0.27	0.787
Substrate	22.058	9.000	2.45	0.016
BC	-0.0006505	0.0007353	-0.88	0.378
BD	-0.2151	0.1706	-1.26	0.210
CD	-0.001604	0.001970	-0.81	0.417
BE	-0.02119	0.06185	-0.34	0.733
CE	-0.000078	0.001014	-0.08	0.939
BF	-0.4176	0.3241	-1.29	0.201
CF	-0.003929	0.004539	-0.87	0.389
BCD	0.00009375	0.00007860	1.19	0.236
BCE	0.00000562	0.00003300	0.17	0.865
BCF	0.0001267	0.0001611	0.79	0.433

S = 1.78952 R-Sq = 93.8% R-Sq(adj) = 92.9%

Analysis of Variance

Source	DF	SS	MS	F	P
Regression	15	5064.05	337.60	105.42	0.000
Residual Error	104	333.05	3.20		
Total	119	5397.10			

Source	DF	Seq SS
Gas Flow Rate	1	52.12
Laser Power	1	1137.65
Conc. Of Ti	1	2463.39
Traverse Rate	1	86.86
Substrate	1	1168.62
BC	1	16.35
BD	1	52.86
CD	1	0.02
BE	1	2.42
CE	1	1.04
BF	1	67.44
CF	1	0.10
BCD	1	12.94
BCE	1	0.23
BCF	1	1.98

Unusual Observations

Gas Flow						
Obs	Rate	Hardness	Fit	SE Fit	Residual	St Resid
5	10.0	64.000	67.400	0.800	-3.400	-2.12R
26	34.0	72.000	75.800	0.800	-3.800	-2.37R
83	10.0	84.000	87.758	0.410	-3.758	-2.16R
99	34.0	88.000	84.362	0.231	3.638	2.05R
104	42.0	87.000	83.230	0.251	3.770	2.13R
105	42.0	87.000	83.230	0.251	3.770	2.13R
114	58.0	77.000	80.967	0.391	-3.967	-2.27R
118	66.0	76.000	79.835	0.483	-3.835	-2.23R

R denotes an observation with a large standardized residual.

Regression Analysis: Hardness versus Gas Flow Rate, Laser Power, ...

* DE is highly correlated with other X variables
 * DE has been removed from the equation.
 * DF is highly correlated with other X variables
 * DF has been removed from the equation.
 * EF is highly correlated with other X variables
 * EF has been removed from the equation.
 * BDF is highly correlated with other X variables
 * BDF has been removed from the equation.
 * CDF is highly correlated with other X variables
 * CDF has been removed from the equation.
 * BEF is highly correlated with other X variables
 * BEF has been removed from the equation.
 * CEF is highly correlated with other X variables
 * CEF has been removed from the equation.
 * DEF is highly correlated with other X variables
 * DEF has been removed from the equation.
 * BCDF is highly correlated with other X variables
 * BCDF has been removed from the equation.
 * BCEF is highly correlated with other X variables
 * BCEF has been removed from the equation.
 * BDEF is highly correlated with other X variables
 * BDEF has been removed from the equation.
 * CDEF is highly correlated with other X variables
 * CDEF has been removed from the equation.
 * BCDEF is highly correlated with other X variables
 * BCDEF has been removed from the equation.

The regression equation is

Hardness = 26.8 + 1.25 Gas Flow Rate + 0.00905 Laser Power + 7.08 Conc.
 Of Ti + 0.51 Traverse Rate + 22.1 Substrate - 0.000538 BC - 0.130 BD -
 0.00129 CD - 0.418 BF - 0.00393 CF + 0.000071 BCD - 0.0042 BDE
 - 0.000016 CDE + 0.000127 BCF + 0.000001 BCDE

Predictor	Coef	SE Coef	T	P
Constant	26.76	41.94	0.64	0.525
Gas Flow Rate	1.2457	0.7035	1.77	0.080
Laser Power	0.009049	0.008121	1.11	0.268
Conc. Of Ti	7.084	4.276	1.66	0.101
Traverse Rate	0.515	1.903	0.27	0.787
Substrate	22.058	9.000	2.45	0.016
BC	-0.0005382	0.0003241	-1.66	0.100
BD	-0.1303	0.3005	-0.43	0.665
CD	-0.001291	0.004510	-0.29	0.775
BF	-0.4176	0.3241	-1.29	0.201
CF	-0.003929	0.004539	-0.87	0.389
BCD	0.0000713	0.0001536	0.46	0.644
BDE	-0.00424	0.01237	-0.34	0.733
CDE	-0.0000157	0.0002029	-0.08	0.939
BCF	0.0001267	0.0001611	0.79	0.433
BCDE	0.00000112	0.00000660	0.17	0.865

S = 1.78952 R-Sq = 93.8% R-Sq(adj) = 92.9%

Analysis of Variance

Source	DF	SS	MS	F	P
Regression	15	5064.05	337.60	105.42	0.000
Residual Error	104	333.05	3.20		
Total	119	5397.10			

Source	DF	Seq SS
Gas Flow Rate	1	52.12
Laser Power	1	1137.65
Conc. Of Ti	1	2463.39
Traverse Rate	1	86.86
Substrate	1	1168.62
BC	1	16.35
BD	1	52.86
CD	1	0.02
BF	1	63.47
CF	1	0.36
BCD	1	13.21
BDE	1	6.77
CDE	1	0.15
BCF	1	2.12
BCDE	1	0.09

Unusual Observations

Obs	Gas Flow Rate	Hardness	Fit	SE Fit	Residual	St Resid
5	10.0	64.000	67.400	0.800	-3.400	-2.12R
26	34.0	72.000	75.800	0.800	-3.800	-2.37R
83	10.0	84.000	87.758	0.410	-3.758	-2.16R
99	34.0	88.000	84.362	0.231	3.638	2.05R
104	42.0	87.000	83.230	0.251	3.770	2.13R
105	42.0	87.000	83.230	0.251	3.770	2.13R
114	58.0	77.000	80.967	0.391	-3.967	-2.27R
118	66.0	76.000	79.835	0.483	-3.835	-2.23R

R denotes an observation with a large standardized residual.

Regression Analysis: Hardness versus Gas Flow Rate, Laser Power, ...

- * DE is highly correlated with other X variables
- * DE has been removed from the equation.
- * DF is highly correlated with other X variables
- * DF has been removed from the equation.
- * EF is highly correlated with other X variables
- * EF has been removed from the equation.
- * BDF is highly correlated with other X variables
- * BDF has been removed from the equation.

* CDF is highly correlated with other X variables
 * CDF has been removed from the equation.
 * DEF is highly correlated with other X variables
 * DEF has been removed from the equation.
 * BCDF is highly correlated with other X variables
 * BCDF has been removed from the equation.
 * BDEF is highly correlated with other X variables
 * BDEF has been removed from the equation.
 * CDEF is highly correlated with other X variables
 * CDEF has been removed from the equation.
 * BCDEF is highly correlated with other X variables
 * BCDEF has been removed from the equation.

The regression equation is

Hardness = 41.8 + 0.385 Gas Flow Rate + 0.00263 Laser Power + 3.34

Conc. Of Ti

+ 0.51 Traverse Rate + 25.8 Substrate - 0.000163 BC - 0.21

BF

- 0.0040 CF + 0.000108 BCF - 0.0212 BEF - 0.00008 CEF +

0.000006 BCEF

Predictor	Coef	SE Coef	T	P
Constant	41.75	38.13	1.09	0.276
Gas Flow Rate	0.3852	0.1698	2.27	0.025
Laser Power	0.002632	0.001960	1.34	0.182
Conc. Of Ti	3.3375	0.2816	11.85	0.000
Traverse Rate	0.515	1.894	0.27	0.786
Substrate	25.805	7.887	3.27	0.001
BC	-0.00016319	0.00007822	-2.09	0.039
BF	-0.209	1.104	-0.19	0.850
CF	-0.00397	0.01796	-0.22	0.826
BCF	0.0001081	0.0005860	0.18	0.854
BEF	-0.02119	0.06155	-0.34	0.731
CEF	-0.000078	0.001009	-0.08	0.938
BCEF	0.00000562	0.00003284	0.17	0.865

S = 1.78104 R-Sq = 93.7% R-Sq(adj) = 93.0%

Analysis of Variance

Source	DF	SS	MS	F	P
Regression	12	5057.68	421.47	132.87	0.000
Residual Error	107	339.42	3.17		
Total	119	5397.10			

Source	DF	Seq SS
Gas Flow Rate	1	52.12
Laser Power	1	1137.65
Conc. Of Ti	1	2463.39
Traverse Rate	1	86.86
Substrate	1	1168.62
BC	1	16.35
BF	1	114.88

CF	1	0.02
BCF	1	10.93
BEF	1	6.62
CEF	1	0.15
BCEF	1	0.09

Unusual Observations

Gas Flow						
Obs	Rate	Hardness	Fit	SE Fit	Residual	St Resid
5	10.0	64.000	67.763	0.630	-3.763	-2.26R
26	34.0	72.000	76.438	0.630	-4.438	-2.66R
83	10.0	84.000	87.758	0.408	-3.758	-2.17R
99	34.0	88.000	84.362	0.230	3.638	2.06R
104	42.0	87.000	83.230	0.250	3.770	2.14R
105	42.0	87.000	83.230	0.250	3.770	2.14R
114	58.0	77.000	80.967	0.389	-3.967	-2.28R
118	66.0	76.000	79.835	0.481	-3.835	-2.24R

R denotes an observation with a large standardized residual.

Regression Analysis: Hardness versus Gas Flow Rate, Laser Power, ...

- * DE is highly correlated with other X variables
- * DE has been removed from the equation.
- * DF is highly correlated with other X variables
- * DF has been removed from the equation.
- * EF is highly correlated with other X variables
- * EF has been removed from the equation.
- * DEF is highly correlated with other X variables
- * DEF has been removed from the equation.

The regression equation is

Hardness = 41.8 + 0.385 Gas Flow Rate + 0.00263 Laser Power + 3.34
Conc. Of Ti

+ 0.51 Traverse Rate + 25.8 Substrate - 0.000163 BC - 0.042

BDF

- 0.00079 CDF + 0.000022 BCDF - 0.0042 BDEF - 0.000016 CDEF
+ 0.000001 BCDEF

Predictor	Coef	SE Coef	T	P
Constant	41.75	38.13	1.09	0.276
Gas Flow Rate	0.3852	0.1698	2.27	0.025
Laser Power	0.002632	0.001960	1.34	0.182
Conc. Of Ti	3.3375	0.2816	11.85	0.000
Traverse Rate	0.515	1.894	0.27	0.786
Substrate	25.805	7.887	3.27	0.001
BC	-0.00016319	0.00007822	-2.09	0.039
BDF	-0.0418	0.2209	-0.19	0.850
CDF	-0.000793	0.003591	-0.22	0.826
BCDF	0.0000216	0.0001172	0.18	0.854
BDEF	-0.00424	0.01231	-0.34	0.731
CDEF	-0.0000157	0.0002019	-0.08	0.938
BCDEF	0.00000112	0.00000657	0.17	0.865

S = 1.78104 R-Sq = 93.7% R-Sq(adj) = 93.0%

Analysis of Variance

Source	DF	SS	MS	F	P
Regression	12	5057.68	421.47	132.87	0.000
Residual Error	107	339.42	3.17		
Total	119	5397.10			

Source	DF	Seq SS
Gas Flow Rate	1	52.12
Laser Power	1	1137.65
Conc. Of Ti	1	2463.39
Traverse Rate	1	86.86
Substrate	1	1168.62
BC	1	16.35
BDF	1	114.88
CDF	1	0.02
BCDF	1	10.93
BDEF	1	6.62
CDEF	1	0.15
BCDEF	1	0.09

Unusual Observations

	Gas Flow	Hardness	Fit	SE Fit	Residual	St Resid
Obs	Rate					
5	10.0	64.000	67.763	0.630	-3.763	-2.26R
26	34.0	72.000	76.438	0.630	-4.438	-2.66R
83	10.0	84.000	87.758	0.408	-3.758	-2.17R
99	34.0	88.000	84.362	0.230	3.638	2.06R
104	42.0	87.000	83.230	0.250	3.770	2.14R
105	42.0	87.000	83.230	0.250	3.770	2.14R
114	58.0	77.000	80.967	0.389	-3.967	-2.28R
118	66.0	76.000	79.835	0.481	-3.835	-2.24R

R denotes an observation with a large standardized residual.

Regression Analysis: Hardness versus Gas Flow Rate, Laser Power, ...

- * DE is highly correlated with other X variables
- * DE has been removed from the equation.
- * DF is highly correlated with other X variables
- * DF has been removed from the equation.
- * EF is highly correlated with other X variables
- * EF has been removed from the equation.
- * DEF is highly correlated with other X variables
- * DEF has been removed from the equation.

The regression equation is

Hardness = 68.0 - 0.300 Gas Flow Rate - 0.00388 Laser Power + 3.34
 Conc. Of Ti
 + 0.017 Traverse Rate + 9.96 Substrate + 0.000106 BC

Predictor	Coef	SE Coef	T	P
Constant	68.045	3.934	17.30	0.000
Gas Flow Rate	-0.2999	0.1037	-2.89	0.005
Laser Power	-0.003876	0.001554	-2.49	0.014
Conc. Of Ti	3.3375	0.3232	10.33	0.000
Traverse Rate	0.0168	0.1069	0.16	0.875
Substrate	9.9608	0.5962	16.71	0.000
BC	0.00010598	0.00005358	1.98	0.050

S = 2.04398 R-Sq = 91.3% R-Sq(adj) = 90.8%

Analysis of Variance

Source	DF	SS	MS	F	P
Regression	6	4925.00	820.83	196.47	0.000
Residual Error	113	472.10	4.18		
Total	119	5397.10			

Source	DF	Seq SS
Gas Flow Rate	1	52.12
Laser Power	1	1137.65
Conc. Of Ti	1	2463.39
Traverse Rate	1	86.86
Substrate	1	1168.62
BC	1	16.35

Unusual Observations

Obs	Gas Flow Rate	Hardness	Fit	SE Fit	Residual	St Resid
5	10.0	64.000	70.184	0.543	-6.184	-3.14R
7	34.0	72.000	67.692	0.533	4.308	2.18R
30	34.0	78.500	74.367	0.533	4.133	2.09R
114	58.0	77.000	81.837	0.406	-4.837	-2.41R
118	66.0	76.000	81.006	0.492	-5.006	-2.52R
120	66.0	77.000	81.006	0.492	-4.006	-2.02R

R denotes an observation with a large standardized residual.

Regression Analysis: Hardness versus Gas Flow Rate, Laser Power, ...

- * DF is highly correlated with other X variables
- * DF has been removed from the equation.

The regression equation is

Hardness = 68.4 - 0.299 Gas Flow Rate - 0.00387 Laser Power + 3.34
 Conc. Of Ti
 + 9.94 Substrate + 0.000106 BC

Predictor	Coef	SE Coef	T	P
Constant	68.358	3.376	20.25	0.000
Gas Flow Rate	-0.2988	0.1030	-2.90	0.004
Laser Power	-0.003868	0.001546	-2.50	0.014
Conc. Of Ti	3.3375	0.3218	10.37	0.000
Substrate	9.9360	0.5723	17.36	0.000
BC	0.00010557	0.00005328	1.98	0.050

S = 2.03521 R-Sq = 91.3% R-Sq(adj) = 90.9%

Analysis of Variance

Source	DF	SS	MS	F	P
Regression	5	4924.90	984.98	237.80	0.000
Residual Error	114	472.20	4.14		
Total	119	5397.10			

Source	DF	Seq SS
Gas Flow Rate	1	52.12
Laser Power	1	1137.65
Conc. Of Ti	1	2463.39
Substrate	1	1255.47
BC	1	16.26

Unusual Observations

	Gas Flow					
Obs	Rate	Hardness	Fit	SE Fit	Residual	St Resid
5	10.0	64.000	70.180	0.540	-6.180	-3.15R
7	34.0	72.000	67.697	0.530	4.303	2.19R
30	34.0	78.500	74.372	0.530	4.128	2.10R
114	58.0	77.000	81.824	0.396	-4.824	-2.42R
118	66.0	76.000	80.996	0.485	-4.996	-2.53R
120	66.0	77.000	80.996	0.485	-3.996	-2.02R

R denotes an observation with a large standardized residual.

Regression Analysis: Hardness versus Gas Flow Rate, Laser Power, ...

The regression equation is
 Hardness = 68.4 - 0.299 Gas Flow Rate - 0.00387 Laser Power + 3.34
 Conc. Of Ti
 + 9.94 Substrate + 0.000106 BC

Predictor	Coef	SE Coef	T	P
-----------	------	---------	---	---

Constant	68.358	3.376	20.25	0.000
Gas Flow Rate	-0.2988	0.1030	-2.90	0.004
Laser Power	-0.003868	0.001546	-2.50	0.014
Conc. Of Ti	3.3375	0.3218	10.37	0.000
Substrate	9.9360	0.5723	17.36	0.000
BC	0.00010557	0.00005328	1.98	0.050

S = 2.03521 R-Sq = 91.3% R-Sq(adj) = 90.9%

Analysis of Variance

Source	DF	SS	MS	F	P
Regression	5	4924.90	984.98	237.80	0.000
Residual Error	114	472.20	4.14		
Total	119	5397.10			

Source	DF	Seq SS
Gas Flow Rate	1	52.12
Laser Power	1	1137.65
Conc. Of Ti	1	2463.39
Substrate	1	1255.47
BC	1	16.26

Unusual Observations

Gas Flow						
Obs	Rate	Hardness	Fit	SE Fit	Residual	St Resid
5	10.0	64.000	70.180	0.540	-6.180	-3.15R
7	34.0	72.000	67.697	0.530	4.303	2.19R
30	34.0	78.500	74.372	0.530	4.128	2.10R
114	58.0	77.000	81.824	0.396	-4.824	-2.42R
118	66.0	76.000	80.996	0.485	-4.996	-2.53R
120	66.0	77.000	80.996	0.485	-3.996	-2.02R

R denotes an observation with a large standardized residual.

Regression Analysis: Hardness versus Gas Flow Rate, Laser Power, ...

The regression equation is

Hardness = 68.4 - 0.299 Gas Flow Rate - 0.00387 Laser Power + 3.34
Conc. Of Ti
+ 9.94 Substrate + 0.000106 BC

Predictor	Coef	SE Coef	T	P
Constant	68.358	3.376	20.25	0.000
Gas Flow Rate	-0.2988	0.1030	-2.90	0.004
Laser Power	-0.003868	0.001546	-2.50	0.014
Conc. Of Ti	3.3375	0.3218	10.37	0.000
Substrate	9.9360	0.5723	17.36	0.000
BC	0.00010557	0.00005328	1.98	0.050

S = 2.03521 R-Sq = 91.3% R-Sq(adj) = 90.9%

Analysis of Variance

Source	DF	SS	MS	F	P
Regression	5	4924.90	984.98	237.80	0.000
Residual Error	114	472.20	4.14		
Total	119	5397.10			

Source	DF	Seq SS
Gas Flow Rate	1	52.12
Laser Power	1	1137.65
Conc. Of Ti	1	2463.39
Substrate	1	1255.47
BC	1	16.26

Unusual Observations

	Gas Flow	Rate	Hardness	Fit	SE Fit	Residual	St Resid
Obs							
5	10.0		64.000	70.180	0.540	-6.180	-3.15R
7	34.0		72.000	67.697	0.530	4.303	2.19R
30	34.0		78.500	74.372	0.530	4.128	2.10R
114	58.0		77.000	81.824	0.396	-4.824	-2.42R
118	66.0		76.000	80.996	0.485	-4.996	-2.53R
120	66.0		77.000	80.996	0.485	-3.996	-2.02R

R denotes an observation with a large standardized residual.

Residual Plots for Hardness

APPENDIX III

DMD Analog Settings vs. Real World Values

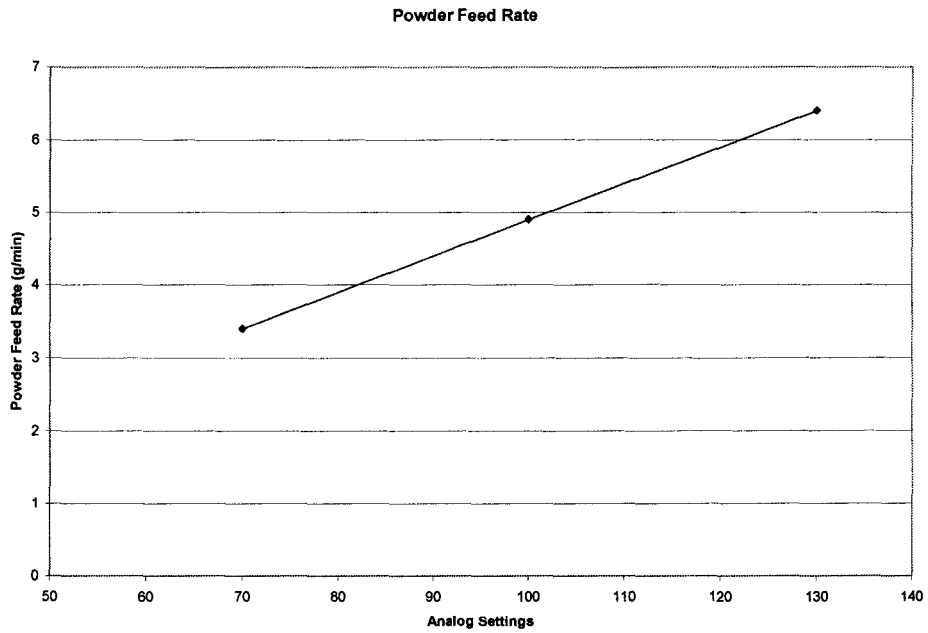


Figure 23. Powder Feed Rate Values

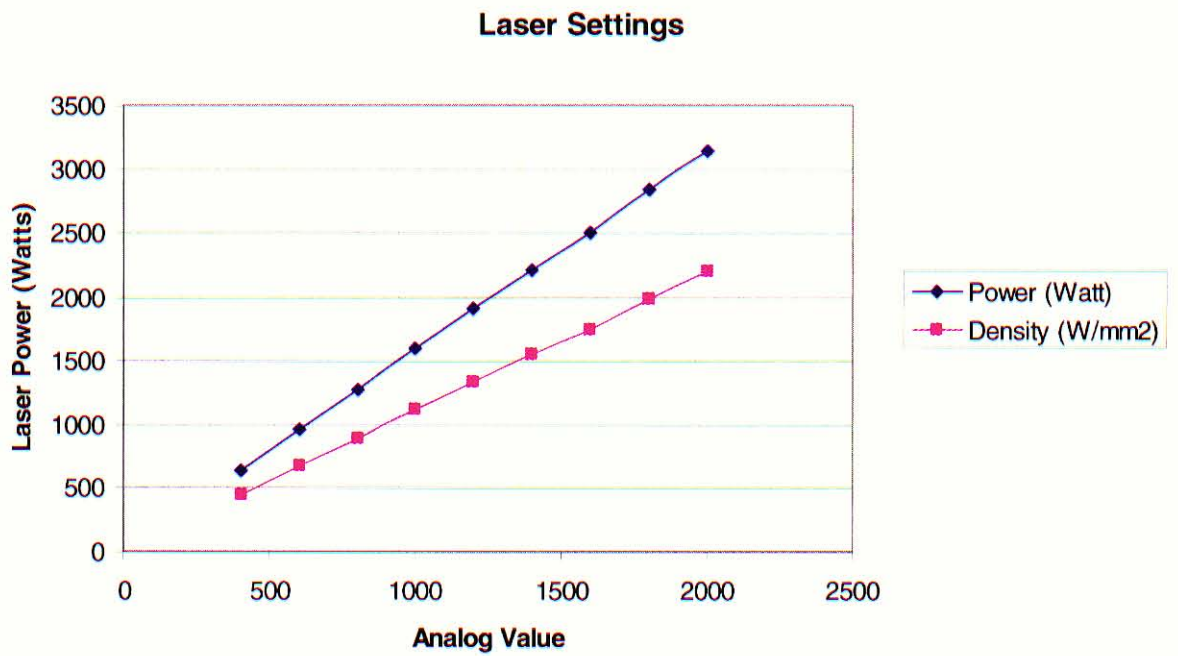


Figure 24. Values for Laser Power

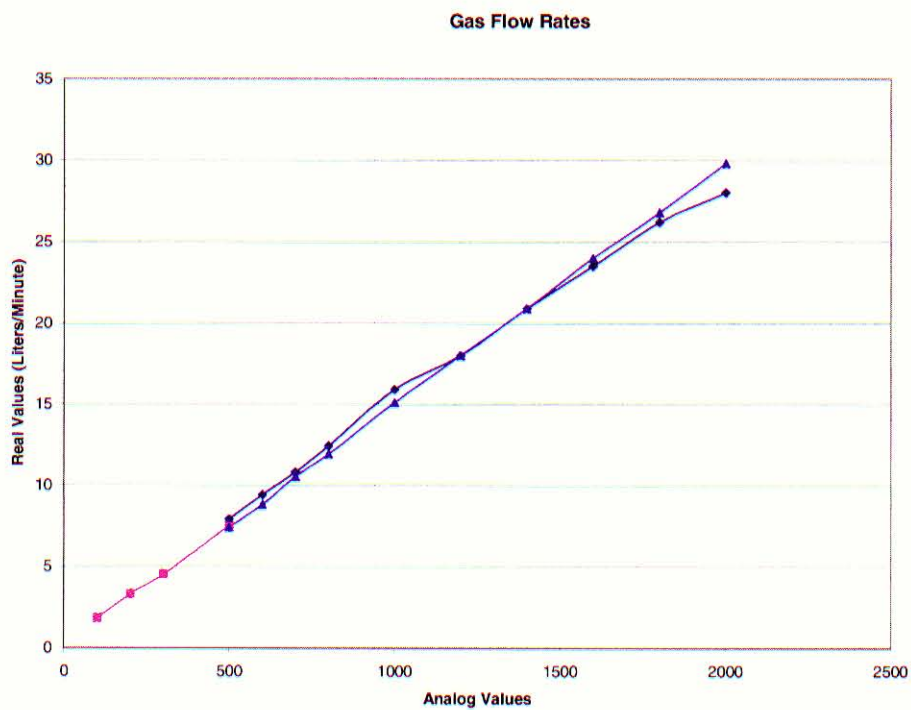


Figure 25. Values for Gas Flow Rate

APPENDIX IV

Gage Reliability and Repeatability for the Rockwell Hardness Tester

Table 10. Gage Reliability and Repeatability for the Rockwell Hardness Tester

	Operator 1 (SJG)				Operator 2 (APD)			
Sample #	Run 1	Run 2	Xbar	R	Run 1	Run 2	Xbar	R
1	23	25	24	2	25.5	25	25.25	0.5
2	24	25	24.5	1	24	25	24.5	1
3	25	25	25	0	25	27	26	2
4	24.5	25	24.75	0.5	25.5	25	25.25	0.5
5	25	24.5	24.75	0.5	25	25.5	25.25	0.5
Melt Flow rate in g/10min			Xdoublebar	Rbar			Xdoublebar	Rbar
			24.6	0.8			25.25	0.9

For sample size 5,
d=2.326

Rdoublebar	0.85
Sigma Repeatability	0.37

Rsubx	-0.65
Sigma Reproducibility	-0.28

overall average	24.93
overall std. dev. (sigma total)	0.77

(Sigma gage) ²	0.21
Sigma Gage	0.46

(sigma gage) / (sigma total)	0.60
---------------------------------	------

APPENDIX V

Oxygen Test Results

October 5, 2005

CERTIFIED MATERIAL ANALYSIS

Joseph Vicars
University of Louisville
J.B. Speed Scientific
School

IMR Report Number 200508701

SUMMARY

The results from the oxygen analyses are given in the table below.

PO Number
23049

Date Received
September 21, 2005

CHEMISTRY

Part #

1: Baseline Substrate
2: DMD pure Ni
3: DMD Ni with 3% Ti
A: Ni Powder

Material

Ni alloy and nickel
powder

Sample	O ¹
1	0.006
2	0.15
3	0.046
A	0.084

¹Determined by combustion-infrared absorbance.

Results in weight percent unless otherwise indicated.

Method: ASTM E 1019-03.



Reviewed by
Alexis Puerta, Ph.D.
Research Chemist

Reviewed by
Peter Damian, Manager
Chemistry Department

All procedures were performed in accordance with the IMR Quality Manual, current revision, and related procedures; and the PWA-MCL Manual F-23 and related procedures. The information contained in this test report represents only the material tested and may not be reproduced, except in full, without the written approval of IMR, Inc. IMR, Inc. maintains a quality system in compliance with the ISO/IEC 17025:1999 and is accredited by the American Association for Laboratory Accreditation (A2LA), certificates #1140.01 and #1140.02. IMR, Inc.'s liability to the customer or any third party is limited to the amount charged for services provided. All samples will be retained for a minimum of 6 months and may be destroyed thereafter unless otherwise specified by the customer. The recording of false, fictitious, or fraudulent statements or entries on this document may be punished as a felony under federal statutes. Tensile testing was not performed in accordance with NADCAP requirements (including the strain rate used), but does conform to A2LA and ASTM E8 requirements.

APPENDIX VI

Recipes for All DMD Experiment

Run #	1	2	3	4
Recipie I.D. #	1.561	1.561	1.561	1.561
Shaping gas flow Ar	2000	1000	1500	1500
Cover gas flow Ar	100	100	100	100
Carrier Flow Ar	200	200	200	200
Carrier Flow He	50	50	50	50
Nozzle Gas Flow Ar	1300	650	975	975
Nozzle Gas Flow He	500	250	375	375
Hopper Rate	100	100	100	100
Measured Rate	4.85	4.85	4.85	4.85
Control Laser Power	1400	1400	1400	1400
LCD Laser Power	2130	2130	2130	2174
Laser Freq	1280	1280	1280	1280
CNC Vel (in/min)	20	20	20	20
Material	Ni 56C-NS	Ni 56C-NS	Ni 56C-NS	Ni 56C-NS
Box Gas Used ? (yes at 10 psi unless otherwise)	NO	NO	NO	YES @ 3 PSI
Comments	Noticable Porosity Build HT = .043 Color - Dull, Silver	Less Porosity Than #1 Build HT = .04 Color - Brown, Blue	Less Porosity Than #1 Build HT = .036 Color = Light Blue	Less Porosity Than #1 but still noticable Build HT = .033 Color Dark Blue, Brown

[illegible]

Run #	16-2	17	18	19	20	21	22	23
Recipe I.D. #	1.561	1.561	1.561	1.561	1.561	1.561	1.561	1.561
Shaping gas flow Ar	1500	1500	1500	2000	2000	2000	2000	2000
Cover gas flow Ar	100	100	100	100	100	100	100	100
Carrier Flow Ar	200	200	200	200	200	200	200	200
Carrier Flow He	50	50	50	50	50	50	50	50
Nozzle Gas Flow Ar	975	975	975	1300	1300	1300	1300	1300
Nozzle Gas Flow He	375	375	375	500	500	500	500	500
Hopper Rate	100	100	100	100	100	100	100	100
Measured Rate	4.75	4.75	5	5	5	5	5	5
Control Laser Power	1000	1400	1400	1400	1400	1400	1400	1400
LCD Laser Power	1600	2150	2150	2150	2150	2150	2150	2150
Laser Freq	1280	1280	1280	1280	1280	1280	1280	1280
CNC Vel (in/min)	20	10	20	20	20	20	20	20
Material	Ni 56C-NS	Ni 56C-NS	Ni 56C-NS	Ni 56C-NS	Ni 56C-NS	Ni 56C-NS	Ni 56C-NS	Ni 56C-NS
Box Gas Used ? (yes at 10 psi unless otherwise)	NO	NO	NO	NO	NO	NO	NO	NO
Comments		Feed Rapid 50%	Pre-Heat Controlled Cool Down From 380 100% Feed	Pre-Heat Controlled Cool Down From 380 100% Feed	1 Layer Only No Preheat	2 Layer No Preheat	3 Layer No Preheat	4 Layer No Preheat

Run #	24	25	26	27	28	29	30	31	32
Recipe I.D. #	1.561	1.561	1.561	1.561	1.561	1.561	1.561	1.561	1.561
Shaping gas flow Ar	2000	500	500	500	500	500	500	500	500
Cover gas flow Ar	100	100	100	100	100	100	100	100	100
Carrier Flow Ar	200	200	200	200	200	200	200	200	200
Carrier Flow He	50	50	50	50	50	50	50	50	50
Nozzle Gas Flow Ar	1300	200	200	200	200	200	200	200	200
Nozzle Gas Flow He	500	0	0	0	0	0	0	0	0
Hopper Rate	100	100	100	100	100	100	100	100	100
Measured Rate									
Control Laser Power	1400	1200	800	1000	1000		1200	1400	1400
LCD Laser Power			1322	1609	1615				
Laser Freq	1280	1280	1280	1280	1280	1280	1280	1280	1280
CNC Vel (in/min)	20	15	15	15	15	10	20	20	20
Material	Ni 56C-NS	Ni 56C-NS	Ni 56C-NS	Ni 56C-NS	Nickel 99.9%	Nickel 99.9%	Nickel 99.9%	Nickel 99.9%	Ni 56C-3%Ti
Box Gas Used ? (yes at 10 psi unless otherwise stated)	NO	NO	NO	NO	NO	NO	NO	NO	NO
Comments				Pre-heat 350°F					

Run #	33	34	35	36	37	38	39	40	41
Recipie I.D. #	1.561	1.561	1.561	1.561	1.561	1.561	1.561	1.561	1.561
Shaping gas flow Ar	500	500	500	500	1000	750	500	500	500
Cover gas flow Ar	100	100	100	100	100	100	100	100	100
Carrier Flow Ar	200	200	200	200	200	200	200	200	200
Carrier Flow He	50	50	50	50	50	50	50	50	50
Nozzle Gas Flow Ar	200	200	200	200	100	750	500	200	200
Nozzle Gas Flow He	0	0	0	0	300	200	100	0	0
Hopper Rate	100	100	100	100	100	100	100	100	100
Measured Rate					4.6				
Control Laser Power	1200	1600	1600	1400	1200	1200	1200	1200	1200
LCD Laser Power		2200	2200		1900				1850
Laser Freq	1280	1280	1280	1280	1280	1280	1280	1280	1280
CNC Vel (in/min)	15	25	25	20	15	15	15	15	15
Material	Ni 56C-3%Ti	Ni 56C-3%Ti	Ni 56C-3%Al	Ni 56C-3%Al	Ni 56C-3%Ti	Ni 56C-3%Ti	Ni 56C-3%Ti	Ni 56C-3%Ti	Ni 56C-3%Ti
Box Gas Used ? (yes at 10 psi unless otherwise stated)	NO	NO	NO	NO	NO	NO	NO	NO	NO
Comments			Obvious Seperation Seen in Powder						

Run #	42	43	44	45	46	47	48	49	50
Recipie I.D. #	1.561	1.561	1.561	1.561	1.561	1.561	1.561	1.561	1.561
Shaping gas flow Ar	1000	500	1000	500	1000	500	1000	500	1200
Cover gas flow Ar	100	100	100	100	100	100	100	100	100
Carrier Flow Ar	200	200	200	200	200	200	200	200	200
Carrier Flow He	50	50	50	50	50	50	50	50	50
Nozzle Gas Flow Ar	1000	200	1000	200	1000	200	1000	500	1200
Nozzle Gas Flow He	300	0	300	0	300	0	300	100	300
Hopper Rate	100	100	100	100	100	100	100	100	100
Measured Rate								4.8	
Control Laser Power	1200	1600	1600	1200	1200	1600	1600	1100	1100
LCD Laser Power	1890	2450	2455					1570	
Laser Freq	1280	1280	1280	1280	1280	1280	1280	1280	1280
CNC Vel (in/min)	15	15	15	15	15	15	15	15	15
Material	Ni 56C-3%Ti	Ni 56C-3%Ti	Ni 56C-3%Ti	Ni 56C-5%Ti	Ni 56C-5%Ti	Ni 56C-5%Ti	Ni 56C-5%Ti	Ni 56C-5%Ti	Ni 56C-5%Ti
Box Gas Used ? (yes at 10 psi unless otherwise stated)	NO	NO	NO	NO	NO	NO	NO	NO	NO
Comments						Stopped after 3 Layers High Heat		17 lpm	40 lpm

Run #	51	52	53	54	55	56	57	58	59	60
Recipe I.D. #	1.561	1.561	1.561	1.561	1.561	1.561	1.561	1.561	1.561	1.561
Shaping gas flow Ar	500	1200	500	1200	500	1200	300	550	800	1050
Cover gas flow Ar	100	100	100	100	100	100	100	100	100	100
Carrier Flow Ar	200	200	200	200	200	200	200	200	200	200
Carrier Flow He	50	50	50	50	50	50	50	50	50	50
Nozzle Gas Flow Ar	500	1200	500	1200	500	1200	300	550	800	1050
Nozzle Gas Flow He	100	300	100	300	100	300	50	100	150	200
Hopper Rate	100	100	100	100	100	100	100	100	100	100
Measured Rate										
Control Laser Power	1400	1400	1100	1100	1400	1400	1200	1200	1200	1200
LCD Laser Power	2166									
Laser Freq	1280	1280	1280	1280	1280	1280	1280	1280	1280	1280
CNC Vel (in/min)	15	15	20	20	20	20	20	20	20	20
Material	Ni 56C-5%Ti	Ni 56C-5%Ti	Ni 56C-5%Ti	Ni 56C-5%Ti	Ni 56C-5%Ti	Ni 56C-5%Ti	Ni 56C-5%Ti	Ni 56C-5%Ti	Ni 56C-5%Ti	Ni 56C-5%Ti
Box Gas Used ? (yes at 10 psi unless otherwise stated)	NO	NO	NO	NO	NO	NO	NO	NO	NO	NO
Comments							10 L/MIN	18 L/MIN	26 L/MIN	34 L/MIN

Run #	61	62	63	64	65	66	67	68
Recipie I.D. #	1.561	1.561	1.561	1.561	1.561	1.561	1.561	1.561
Shaping gas flow Ar	1300	1550	1800	2000	800	800	800	800
Cover gas flow Ar	100	100	100	100	100	100	100	100
Carrier Flow Ar	200	200	200	200	200	200	200	200
Carrier Flow He	50	50	50	50	50	50	50	50
Nozzle Gas Flow Ar	1300	1550	1800	2000	800	800	800	800
Nozzle Gas Flow He	250	300	350	400	150	150	150	150
Hopper Rate	100	100	100	100	100	100	100	100
Measured Rate					5	10		
Control Laser Power	1200	1200	1200	1200	1200	1200	1400	1600
LCD Laser Power								
Laser Freq	1280	1280	1280	1280	1280	1280	1280	1280
CNC Vel (in/min)	20	20	20	20	20	20	20	20
Material	Ni 56C-5%Ti	Ni 56C-5%Ti	Ni 56C-5%Ti	Ni 56C-5%Ti	Ni 56C-1%Ti	Ni 56C-1%Ti	Ni 56C-1%Ti	Ni 56C-1%Ti
Box Gas Used ? (yes at 10 psi unless otherwise stated)	NO	NO	NO	NO	NO	NO	NO	NO
Comments	42 L/MIN	50 L/MIN	58 L/MIN	66 L/MIN				

Run #	69	70	71	72	72-2	73	74
Recipe I.D. #	1.561	1.561	1.561	1.561	1.561	1.561	1.561
Shaping gas flow Ar	800	800	800	800	800	800	800
Cover gas flow Ar	100	100	100	100	100	100	100
Carrier Flow Ar	200	200	200	200	200	200	200
Carrier Flow He	50	50	50	50	50	50	50
Nozzle Gas Flow Ar	800	800	800	800	800	800	800
Nozzle Gas Flow He	150	150	150	150	150	150	150
Hopper Rate	100	100	100	100	200	100	100
Measured Rate					10		
Control Laser Power	1800	2000	2000	2000	2000	2000	2000
LCD Laser Power				MAX	MAX		
Laser Freq	1280	1280	1280	1280	1280	1280	1280
CNC Vel (in/min)	20	20	15	10	10	8	10
Material	Ni 56C-1%Ti	Ni 56C-1%Ti	Ni 56C-1%Ti	Ni 56C-1%Ti			
Box Gas Used ? (yes at 10 psi unless otherwise stated)	NO	NO	NO	NO	NO	NO	NO
Comments					Same as #72 but with 3 passes	3 passes	3 passes 3 Anneal passes @ Z = 1.0 Feed = 5 ipm

Note: Increased gas flow rates were needed when nozzle standoff was increased during anneal so that shielding gas can reach the substrate

Run #	75
Recipie I.D. #	1.561
Shaping gas flow Ar	1600/800
Cover gas flow Ar	100
Carrier Flow Ar	200
Carrier Flow He	50
Nozzle Gas Flow Ar	2000/800
Nozzle Gas Flow He	150
Hopper Rate	100
Measured Rate	
Control Laser Power	2000
LCD Laser Power	
Laser Freq	1280
CNC Vel (in/min)	10
Material	
Box Gas Used ? (yes at 10 psi unless otherwise stated)	NO
Comments	3 passes 3 anneal passes Z = 1.0 Feed = 5 ipm increase gas flow on anneal

	Recipie I.D. #	1.561
1	Shaping gas flow Ar	1000
2	Cover gas flow Ar	100
3	Carrier Flow Ar	200
4	Carrier Flow He	50
5	Nozzle Gas Flow Ar	1000
6	Nozzle Gas Flow He	100
7	Hopper Rate	100
8	Measured Rate	4.85
9	Control Laser Power	1400
10	LCD Laser Power	2130
11	Laser Freq	1280
12	CNC Vel (in/min)	20